

RESEARCH ARTICLE

Conserved and divergent functions of Pax6 underlie species-specific neurogenic patterns in the developing amniote brain

Wataru Yamashita¹, Masanori Takahashi², Takako Kikkawa³, Hitoshi Gotoh¹, Noriko Osumi³, Katsuhiko Ono¹ and Tadashi Nomura^{1,*}

ABSTRACT

The evolution of unique organ structures is associated with changes in conserved developmental programs. However, characterizing the functional conservation and variation of homologous transcription factors (TFs) that dictate species-specific cellular dynamics has remained elusive. Here, we dissect shared and divergent functions of Pax6 during amniote brain development. Comparative functional analyses revealed that the neurogenic function of Pax6 is highly conserved in the developing mouse and chick pallium, whereas stage-specific binary functions of Pax6 in neurogenesis are unique to mouse neuronal progenitors, consistent with Pax6-dependent temporal regulation of Notch signaling. Furthermore, we identified that Pax6-dependent enhancer activity of *Dbx1* is extensively conserved between mammals and chick, although *Dbx1* expression in the developing pallium is highly divergent in these species. Our results suggest that spatiotemporal changes in Pax6-dependent regulatory programs contributed to species-specific neurogenic patterns in mammalian and avian lineages, which underlie the morphological divergence of the amniote pallial architectures.

KEY WORDS: Amniote, Evolution, Neurogenesis, Pallium, Pax6, Chick, Mouse

INTRODUCTION

The evolution of animal body structures is accomplished by pronounced changes in conserved developmental programs. Modifications of regulatory gene networks, such as changes in the expression patterns and dosages of transcription factors (TFs), signaling molecules and their downstream targets, contribute to quantitative and qualitative differences in cellular characteristics and dynamics during embryogenesis (Carroll, 2005; Peter and Davidson, 2011). Recent comparative genomics studies have identified significant differences in *cis*- and *trans*-regulatory elements of developmental regulatory genes that are associated with morphological diversity (Heffer et al., 2010; Glassford et al., 2015; Kwon et al., 2016). By contrast, several lines of evidence

demonstrated functional flexibilities of conserved TFs during evolution (Wagner, 2007; Schmidt et al., 2010); however, the variable roles of conserved regulatory genes in taxon- or species-specific developmental programs remain unclear.

The basic patterns of embryonic brain organization are highly conserved in extant vertebrates, whereas the morphology and cellular compositions of mature brains exhibit extensive diversities (Striedter, 2005; Sugahara et al., 2016). In particular, the dorsal part of the telencephalon (the pallium) gives rise to species-specific architecture: the mammalian pallium elaborates the neocortex, which is characterized by horizontal expansion of surface area and a six-layered laminar organization (Nieuwenhuys, 1994). These anatomical hallmarks of the neocortex are constructed by the spatial and temporal regulation of neural progenitor proliferation and differentiation in the developing dorsal pallium; regional and chronological expression of core regulatory genes tightly control the amplification of neural progenitors in the ventricular zone (VZ) and subventricular zone (SVZ) and the sequential production of layer-specific neurons (Götz and Huttner, 2005; Kriegstein et al., 2006). By contrast, the pallium of non-mammalian amniotes, such as reptiles and birds, develops into a three-layered dorsal cortex or Wulst with a tissue slab (Ulinski, 1990; Medina and Reiner, 2000). Furthermore, reptiles and birds have a dorsal ventricular ridge, which is a prominent tissue protrusion at the lateral wall of the cerebral hemisphere, as a derivative of the ventral pallium (VP) (Ulinski, 1983). These morphological differences might be provided by species-specific patterns of progenitor proliferation and neuronal specification in distinct sectors of the embryonic pallium (Suzuki et al., 2012; Nomura et al., 2013; García-Moreno and Molnár, 2015).

Pax6 is a paired domain-containing TF that is expressed in region-specific neural progenitor cells in the developing vertebrate central nervous system (Osumi et al., 2008; Manuel et al., 2015; Ypsilanti and Rubenstein, 2016). Consistently, Pax6 regulates various downstream target genes in response to cell-intrinsic and extrinsic signaling, as well as in response to the levels of Pax6 itself in neuronal progenitors (Holm et al., 2007; Sansom et al., 2009; Thakurela et al., 2016). The expression pattern of Pax6 is highly conserved among vertebrates (Fernandez et al., 1998; Puelles et al., 2000). However, recent studies have demonstrated species-specific functions of Pax6 in the regulation of neural progenitors in the developing mammalian brain (Zhang et al., 2010; Wong et al., 2015), suggesting that evolutionarily variable functions of Pax6 underlie the divergent gene regulations and cellular compositions in the developing pallium (Molnár and Butler, 2002; Aboitiz and Zamorano, 2013). Consistently, Pax6 is required for the establishment of the pallial-subpallial boundary by regulating specific target gene expression in the VP (Yun et al., 2001; Assimacopoulos et al., 2003), a crucial region for the taxon-specific pallial architectures in amniotes (Molnár and Butler, 2002).

¹Developmental Neurobiology, Kyoto Prefectural University of Medicine, INAMORI Memorial Building, 1-5 Shimogamo-hangi cho, Sakyoku, Kyoto, 606-0823, Japan.

²Division of Biology, Center for Molecular Medicine, Jichi Medical University, 3311-1 Yakushiji, Shimotsuke, Tochigi, 329-0498, Japan. ³Department of Developmental Neuroscience, United Center for Advanced Research and Translational Medicine (ART), Tohoku University School of Medicine, 2-1 Seiryo-machi, Aoba-ku, Sendai, Miyagi, 980-8575, Japan.

*Author for correspondence (tadnom@koto.kpu-m.ac.jp)

ID T.N., 0000-0001-8467-9521

This is an Open Access article distributed under the terms of the Creative Commons Attribution License (<http://creativecommons.org/licenses/by/3.0/>), which permits unrestricted use, distribution and reproduction in any medium provided that the original work is properly attributed.

Received 20 September 2017; Accepted 20 March 2018

Here, we report shared and divergent functions of Pax6 in the regulation of species-specific cellular dynamics and downstream target genes in developing mammalian and avian brains. Genetic manipulation of Pax6 functions in the developing chick pallium revealed a conserved role of Pax6 in promoting neuronal differentiation in both mouse and chick. By contrast, Pax6-dependent maintenance of neural progenitors is unique to mammalian corticogenesis, which is consistent with the temporal regulation of Notch signaling activities. Furthermore, we identified that Pax6 has the potential to activate *Dbx1* expression in the developing avian pallium, implicating that gene regulation unique to the mammalian pallium is extensively conserved in non-mammalian brain development. Our results suggest that lineage-specific changes in Pax6-dependent gene regulation contribute to the establishment of the mammalian and avian neurogenic programs, on the basis of conserved regulatory mechanisms derived from common ancestors of amniotes.

RESULTS

Genome editing in chick brain reveals conserved functions of Pax6 in neurogenesis

We chose Pax6 for the analyses of conserved and derived roles of homologous TFs in species-specific brain development because (1) the protein structures and expression patterns of Pax6 are extremely highly conserved among species, (2) other genes with compensatory functions are not expressed in the developing pallium, and (3) downstream target genes have been well-characterized in the developing mouse neocortex. In the developing mouse and chick pallium, Pax6 is highly expressed in the VZ neural progenitors [radial glial cells (RGCs)], although the progenitor compositions and characteristics are not identical in these species (Fig. 1A,B). Notably, despite conservation of Tbr2 (Eomes) expression, Tbr2-positive cells are not basal progenitors but postmitotic neurons in the developing chick pallium (Nomura et al., 2016).

To dissect conserved and variable functions of Pax6 in species-specific brain development, we first performed *in vivo* targeting of chick Pax6 by CRISPR/Cas9-mediated genome editing. We designed three single-guide RNAs (sgRNAs) against the coding region of the chick *Pax6* gene (*Pax6-347*, *Pax6-679* and *Pax6-811*) and cloned them into *pX330* vectors that simultaneously express Cas9 and each sgRNA under the control of different promoters (Fig. 1C, Fig. S1A). These *Pax6* targeting vectors, together with a GFP reporter vector, were electroporated into the pallium of developing chick embryos at embryonic day (E) 4 (which corresponds to Hamburger Hamilton stage 23-24). At 36 h after electroporation, significant decreases in Pax6 expression levels were evident in the neural progenitors transfected with *pX330-Pax6-347*, -679 or -811 compared with those transfected with control plasmid (*pX330* without sgRNA) (Fig. 1D,E, Fig. S1C). High-throughput genome sequencing also confirmed successful insertion-deletion mutations at the target sequences of Pax6 in GFP-positive cells (Fig. S1B).

At 48 h after electroporation, we confirmed that the number of Tbr2-positive or Tbr1-positive postmitotic neurons was dramatically decreased in embryos transfected with *pX330-Pax6-679* or -811 vectors compared with control embryos ($n=3$ embryos; Fig. 1F-I, Fig. S1F,F'). Electroporation of *pX330-Pax6-679* or -811 also induced ectopic expression of Gsh2, a marker for the embryonic subpallium, in the lateral and ventral pallium (Fig. S1D-E'; $n=3$ of 4 embryos). At later embryonic stages, ectopic accumulation of gamma-aminobutyric acid (Gaba)-positive

cells was evident at the VP transfected with *pX330-679*, suggesting that ectopic Gsh2-positive cells differentiate into inhibitory interneurons (Fig. S1J,K). These phenotypes resembled the pallium of *Pax6* mutant mice and rats (Toresson et al., 2000; Yun et al., 2001; Kroll and O'Leary, 2005; Nomura et al., 2006) (Fig. S1H,I). Electroporation of *pX330-Pax6-679* did not increase the number of active caspase 3-positive apoptotic cells (Fig. S1L-N). Thus, Pax6 has a highly conserved function in the differentiation of excitatory neurons from pallial RGCs, despite the divergence of pallial progenitor compositions.

Stage-dependent functions of Pax6 are unique to mammalian neural progenitors

Pax6 plays opposing roles in neurogenesis, either promoting or inhibiting neuronal differentiation in the developing mouse neocortex in stage- and dose-dependent manners (Fukuda et al., 2000; Estivill-Torrus et al., 2002; Sansom et al., 2009; Tuoc et al., 2009). To address whether these binary functions of Pax6 are evolutionarily conserved among amniotes, we performed gain-of-function analyses of Pax6 in chick pallial neural progenitors at different embryonic stages. Expression vectors for *Pax6* and *GFP* were electroporated into the developing chick dorsal pallium at E4 (stage 23-24) or E6 (stage 28-29), which correspond to the early and middle/late stages of neurogenesis, respectively (Fig. 2A,B). At 24 h after electroporation, Pax6 overexpression dramatically increased the proportion of Tbr2-positive cells compared with control embryos transfected with the GFP expression vector, at both early and late stages of neurogenesis (Fig. 2C-F). The Tbr2-positive cells in the chick pallium did not show any proliferative activity, indicating that they are postmitotic neurons, as previously reported (Nomura et al., 2016) (data not shown). Intriguingly, Pax6 overexpression did not alter the proportion of transfected cells in the VZ, suggesting that high-dose Pax6 induced premature neuronal differentiation of progenitors prior to exiting the VZ (Fig. 2G,H).

To examine changes in the frequency of proliferative and neurogenic divisions due to high-dose Pax6, we performed clonal analysis of chick pallial progenitors by co-electroporation of *Cytbow/Nucbow* and Cre recombinase expression vectors, as previously reported (Loulier et al., 2014). At E5, 24 h after electroporation, Pax6 overexpression reduced the proportion of clones containing Sox2-positive progenitors and increased clones with Sox2-negative non-progenitors, suggesting that high-dose Pax6 facilitated symmetric and asymmetric neurogenic divisions (Fig. S2). Thus, consistent with the loss-of-function study, Pax6 plays a crucial role in promoting neuronal differentiation in the developing chick pallium in both the early and late neurogenic periods.

By contrast, in the developing mouse pallium, high levels of Pax6 expression induced distinct outcomes in neuronal progenitors depending on the embryonic stage. In E12.5 mice, overexpression of Pax6 significantly increased the number of Tbr2-positive cells compared with GFP-electroporated control embryos (Fig. 2I,K,M,O). By contrast, in the E14.5 mouse pallium, high-dose Pax6 decreased the number of Tbr2-positive cells at the VZ and SVZ while significantly increasing the proportion of RGCs at the VZ (Fig. 2J, L,N,P).

To examine the proliferative activity of transfected cells in the VZ, we administered EdU 1 h before fixation. In the E12.5 mouse pallium, overexpression of Pax6 significantly decreased the proportion of EdU-positive neural progenitor cells in the VZ (Fig. S3A). However, at middle/later stages of neurogenesis, high-dose Pax6 did not change the proportion of EdU-positive cells in the VZ (Fig. S3B,C),

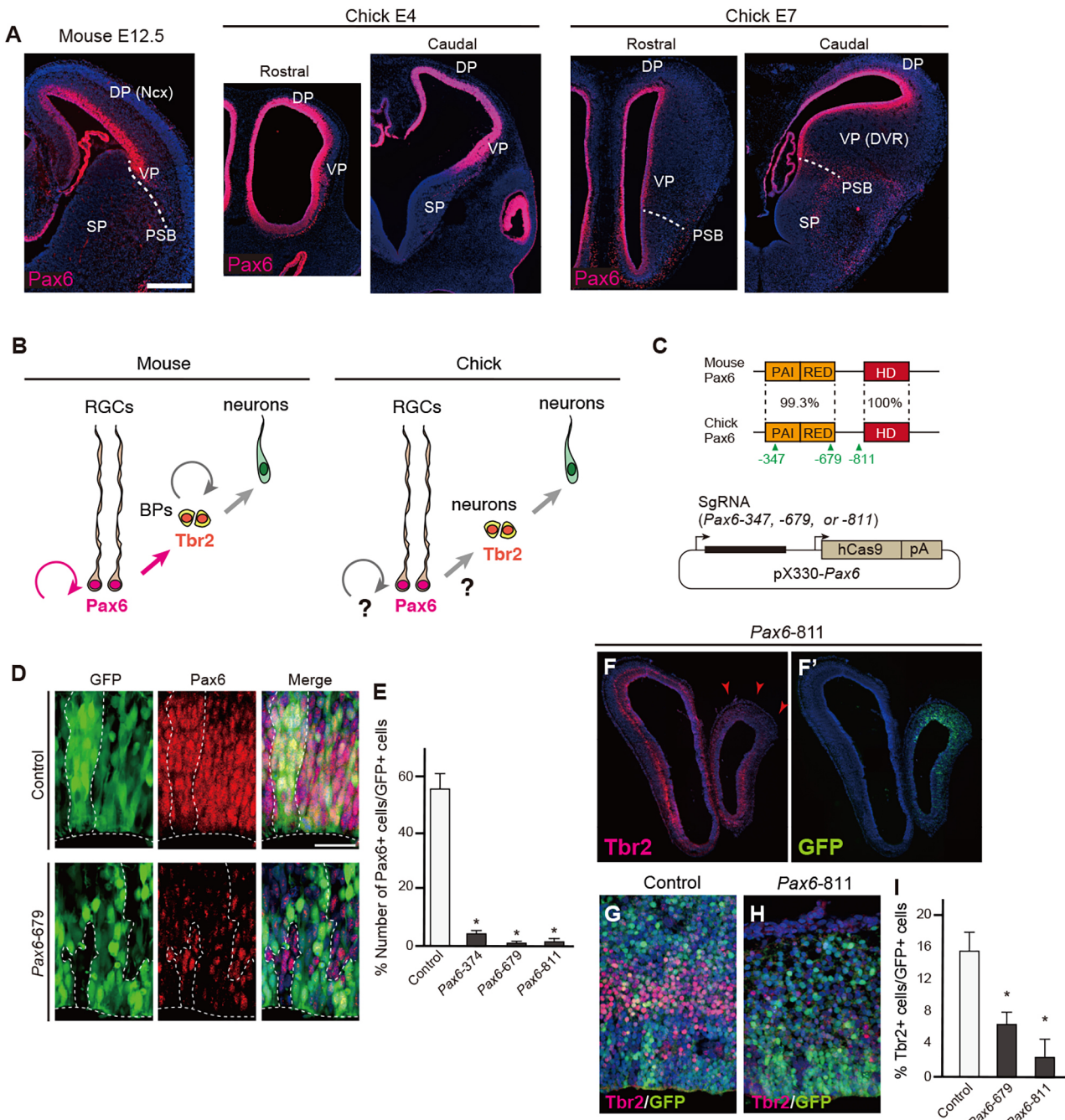


Fig. 1. Targeted deletion of the endogenous *Pax6* gene in the developing chick pallium. (A) Expression patterns of Pax6 protein in mouse (E12.5) or chick (E4 and E7) telencephalon. DP, dorsal pallium; Ncx, neocortex; PSB, pallium-subpallium boundary; SP, subpallium; VP, ventral pallium; DVR, dorsal ventricular ridge. (B) Interspecies differences in mouse and chick pallial neurogenesis. BPs, basal progenitors; RGCs, radial glial cells. (C) (Top) Protein structures of mouse and chick Pax6 showing the percentage identity of domains. The paired domain consists of PAI and RED subdomains; HD, homeodomain. The location of the three sgRNA target sites is indicated. (Bottom) The pX330-Pax6 vector for simultaneous expression of sgRNA and Cas9. (D,E) Electroporation of pX330-based vectors into the developing chick pallium. The number of Pax6-positive cells among GFP-positive cells is significantly decreased by electroporation with pX330-Pax6 vectors (E). Welch's *t*-test, **P*<0.05. Error bars indicate s.e.m. *n*=4. (F-I) Decreased number of Tbr2-positive cells after electroporation of pX330-Pax6. Arrowheads indicate the reduction of Tbr2 expression in the electroporated region. There was no significant difference in the proportion of Tbr2-positive cells between Pax6-679 and -811, indicating that the two sgRNAs were equally efficient in targeting chick Pax6. Error bars indicate s.e.m. *n*=4 for control, *n*=3 for Pax6-679 and -811 samples. Two-tailed Student's *t*-test, **P*<0.05. Scale bars: 200 µm in A; 25 µm in D.

indicating that the proliferative activity of RGCs was maintained by Pax6 overexpression. Similar alterations in progenitor proliferation were also evident in the developing chick pallium by overexpression of Pax6 or a dominant-negative form of Pax6 with the repressor domain (EnR) of the *engrailed* gene (Fig. S3D-F).

These data demonstrated that Pax6 has a conserved function in progenitor proliferation in both the mouse and chick pallium. By contrast, stage-specific binary functions of Pax6 in neuronal differentiation are unique to mouse neocortical neuronal progenitors: high-dose Pax6 accelerates neuronal commitment or

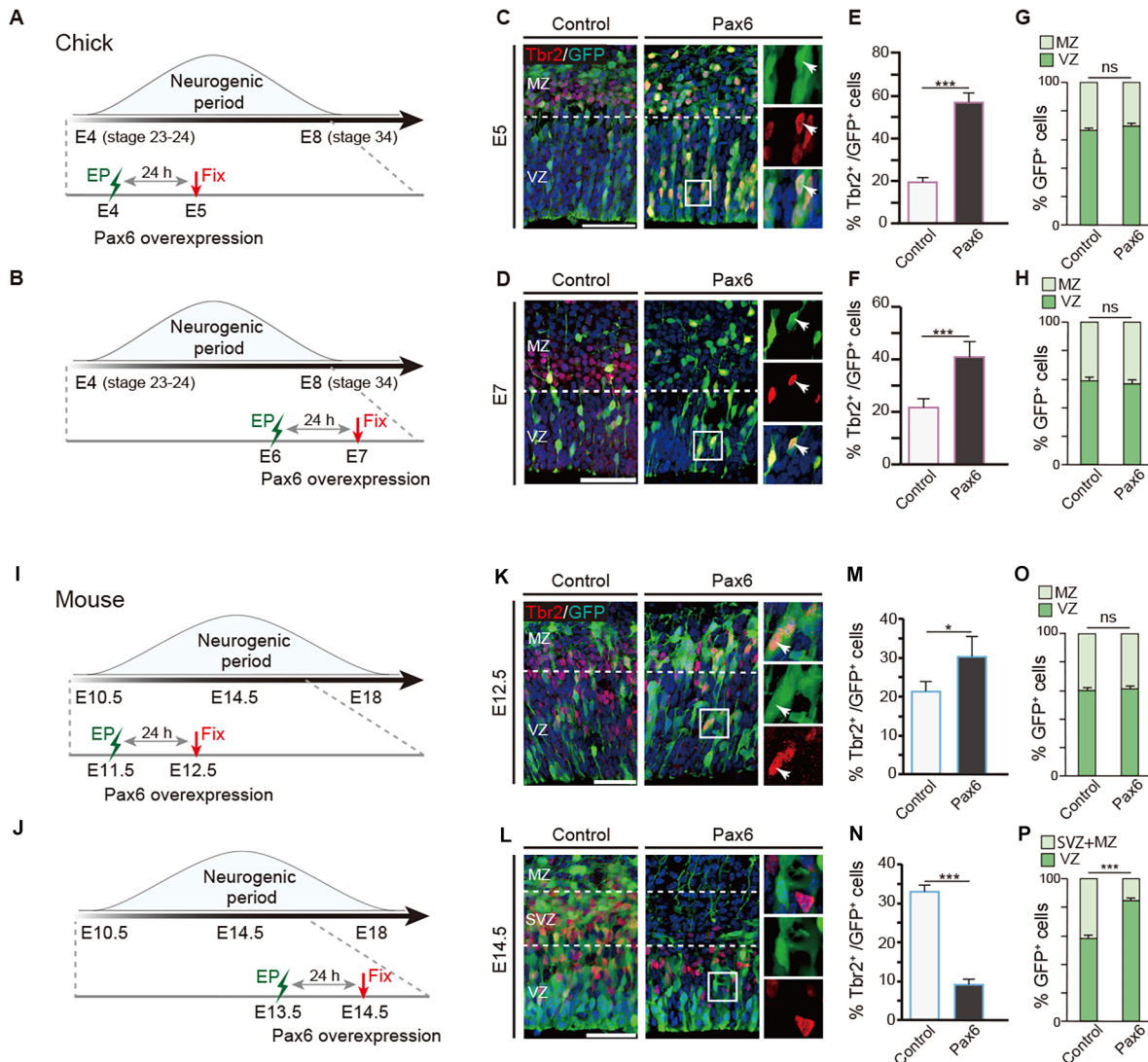


Fig. 2. Interspecies differences in Pax6-dependent pallial neurogenesis between mouse and chick. (A,B) Time schedules of electroporation (EP) in the developing chick pallium. (C-H) Distributions of GFP-positive cells and Tbr2-positive cells in the developing mouse and chick pallium (C,E,G, E5; D,F,H, E7) electroporated with control and Pax6 expression vectors. Pax6 overexpression increases Tbr2-positive cells in both the E5 and E7 chick pallium. Boxed regions are shown at higher magnification on the right, in single channel and merge. Arrowheads indicate cells double positive for Tbr2 and GFP. (I,J) Time schedules of electroporation in the developing mouse neocortex (K,M,O, E12.5; L,N,P, E14.5) electroporated with control and Pax6 expression vectors. Error bars indicate s.e.m. n=6 for each case. Two-tailed Student's t-test, *P<0.05, ***P<0.005; ns, not significant. VZ, ventricular zone; MZ, mantle zone. Scale bars: 50 µm.

differentiation in early stages, whereas it suppresses neuronal differentiation and maintains RGCs after the middle stage of corticogenesis.

Interspecies differences in Pax6-dependent regulation of Notch signaling

To investigate the regulatory mechanisms underlying conserved and variable functions of Pax6 in neurogenesis, we examined gene expression directed by Pax6 in chick pallial progenitors. Quantitative PCR (qPCR) demonstrated that Pax6 overexpression significantly increased the expression of genes encoding Cdk6 and p27^{Kip1} [also known as cyclin-dependent kinase inhibitor 1B (Cdkn1b)] (Fig. 3A), which are regulators of cell cycle progression as downstream targets of Pax6 (Duparc et al., 2007; Sansom et al., 2009). By contrast, high-dose Pax6 decreased the expression of genes encoding Notch1 receptor and Dll1 ligand in the E5 chick

pallium, suggesting that Pax6 overexpression altered Notch signaling activity (Fig. 3B).

To address whether interspecies differences in neurogenic functions of Pax6 are mediated by Notch signaling, we examined Pax6-dependent Notch signaling activity at distinct stages of the developing chick and mouse pallium by transfection of a Notch reporter construct (*4xCSL-luc*) together with the *Pax6* expression vector into isolated neural progenitors (Fig. 3C,D, Fig. S4). After 24 h of transfection, we confirmed that Pax6 overexpression significantly decreased Notch reporter activity in both the early (E4) and late (E7) stages of chick neural progenitors (Fig. 3C). By contrast, Pax6-dependent downregulation of Notch reporter activity was only detected at the early stage (E11) but not at the middle (E13) and late (E15) stages of mouse pallial neural progenitors (Fig. 3D). This is in agreement with the stage-specific changes in neural progenitor states induced by Pax6 overexpression in the developing

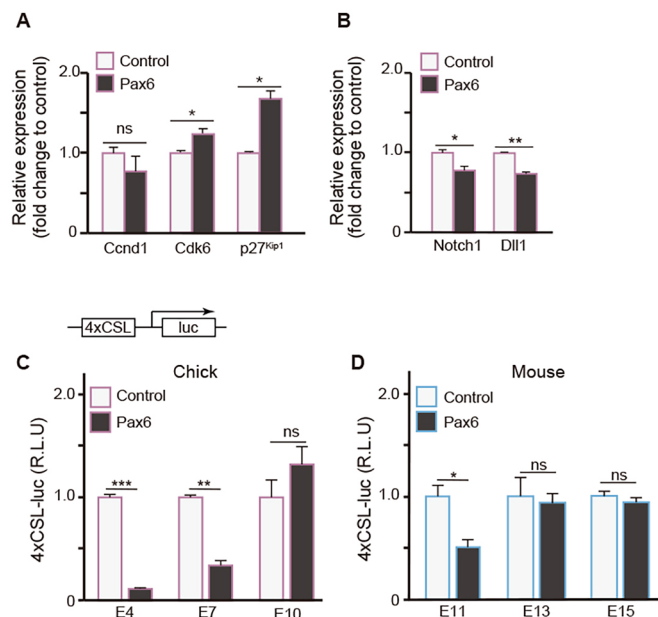


Fig. 3. Temporal differences in Pax6-dependent regulation of Notch signaling. (A,B) mRNA expression levels of *Ccnd1*, *Cdk6*, *p27kip1*, *Notch1* and *Dll1* in E5 chick pallium electroporated with control or Pax6 expression vectors. $n=3$. (C,D) Pax6-dependent temporal changes in Notch reporter (*p4xCSL-luciferase*) activity in neuronal progenitors from different embryonic stages of chick (C) and mouse (D) dorsal pallium. $n=4$ for each case. R.L.U., relative luciferase units. (A-D) Error bars indicate s.e.m. Two-tailed Student's *t*-test, * $P<0.05$, ** $P<0.01$, *** $P<0.005$.

mouse pallium. Notably, a decrease in Notch activity due to Pax6 was not evident in progenitors isolated from the E10 chick pallium (Fig. 3C), when neurogenesis in the developing chick pallium is almost complete (Tsai et al., 1981). This suggests that Pax6-dependent temporal changes in Notch signaling are shared between mouse and chick pallial progenitors, which are uncoupled from the neurogenic periods in each species.

Neural progenitors in the chick VP are less sensitive to high-dose Pax6

Recent studies have shown that spatial differences in pallial neurogenic potentials underlie species-specific neuron subtype compositions (Suzuki et al., 2012; García-Moreno et al., 2018). To examine whether neural progenitors in distinct pallial regions exhibit differential responses to Pax6, we overexpressed Pax6 in the VP of the developing chick brain. At E5, 24 h after electroporation, high-dose Pax6 reduced the proportion of EdU-positive cells in the VP (Fig. S5). By contrast, there was no difference in the number of Tbr2-positive cells in the VP transfected with control and Pax6 expression vectors, suggesting that high-dose Pax6 does not promote neural differentiation in the VP. We also examined Pax6-dependent Notch activity in neurospheres isolated from the chick VP. Pax6 overexpression decreased Notch reporter activity in both the early (E4) and late (E7) stages of VP-derived neural progenitors, but to a lesser degree than in the dorsal pallium-derived neurospheres (Fig. S5).

These results demonstrate regional differences in neural progenitors of the developing chick pallium; neural progenitors derived from the VP are less sensitive to high-dose Pax6 than those from the dorsal pallium with respect to neurogenic potentials. Notably, reduced Notch activity due to Pax6 was not detected in progenitors derived from the E10 VP (Fig. S5), as was also the case

for the dorsal pallium, indicating that Pax6-dependent temporal changes in Notch activity are common characteristics of the dorsal and ventral pallial progenitors in chick.

High-dose Pax6 activates *Dbx1* expression in the developing chick pallium

To further investigate shared and divergent gene regulations directed by Pax6 in an unbiased manner, we performed comprehensive transcriptome analyses for Pax6 target genes in the developing chick pallium. We overexpressed Pax6 in the E5 chick pallium and alterations in mRNA expression profiles were analyzed by RNA sequencing (RNA-seq). As a control, only the GFP reporter vector was introduced into the chick pallium. Pax6 overexpression altered the expression of various genes in the developing chick pallium, including previously reported Pax6 target genes (Table S1). Among these, *Dbx1* exhibited the highest fold change in response to Pax6 overexpression (Table 1). *Dbx1* encodes a homeobox-containing TF that is expressed in the developing mammalian brain and spinal cord under the control of Pax6 (Takahashi and Osumi, 2002; Carney et al., 2009; Numayama-Tsuruta et al., 2010). In the embryonic mouse telencephalon, *Dbx1* is expressed in the septum and VP, and it plays essential roles in the production of specific neuron subtypes including Cajal-Retzius cells and excitatory neurons that migrate into the neocortex or amygdala (Bielle et al., 2005; Hirata et al., 2009; Teissier et al., 2010; Puelles et al., 2016). qPCR analysis confirmed a significant increase in *Dbx1* expression induced by high-dose Pax6 in the developing chick pallium (Fig. 4A). Furthermore, *in situ* hybridization against chick *Dbx1* mRNA demonstrated that Pax6 overexpression induced *Dbx1* expression in the broad area of the chick pallium (Fig. 4B, Fig. S6A,A'). Thus, *Dbx1* is a common downstream target gene of Pax6 in the developing mammalian and avian pallium.

Enhancer activity driving *Dbx1* expression in the VP is highly conserved among amniotes

Notably, the expression pattern of *Dbx1* in the developing pallium is not conserved among amniotes: *Dbx1* is expressed at the septum but is absent at the VP in developing avian brain (Bielle et al., 2005; Nomura et al., 2008), whereas Pax6 is highly expressed in the VP (Fig. 5A). To address whether the Pax6-dependent induction of *Dbx1* in the developing chick pallium is mediated by conserved regulatory mechanisms, we performed comparative functional analyses of mouse and chick *Dbx1* *cis*-regulatory regions. A previous study reported that the distal 3.5 kb of the *Dbx1* regulatory region acts as a *cis*-regulatory module (CRM) that is sufficient to drive specific *Dbx1* expression in the developing mouse pallium

Table 1. Genes upregulated by overexpression of Pax6 in the E5 chick pallium

Gene	Fold change	Gene id
<i>DBX1</i>	126.23	ENSGALG00000003965
<i>CDH12</i>	20.29	ENSGALG00000012941
<i>TLR1LA</i>	18.25	ENSGALG00000017485
<i>MMEL1</i>	15.22	ENSGALG00000001115
<i>PXDNL</i>	14.07	ENSGALG00000005887
<i>DSCAM</i>	14.05	ENSGALG00000016138
<i>7SK (RF00100)</i>	12.10	ENSGALG00000017926
<i>PTPRT</i>	10.32	ENSGALG00000003488
<i>KCNF1</i>	10.08	ENSGALG00000016448
<i>TAC1</i>	8.77	ENSGALG00000009737

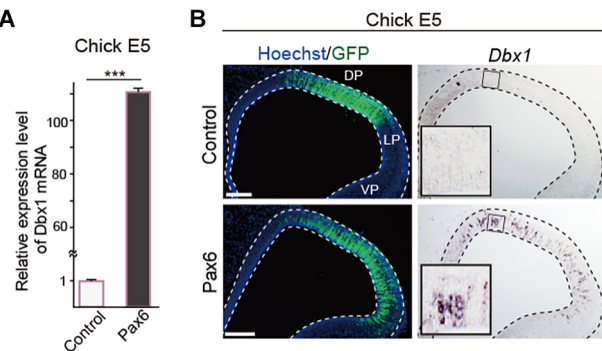


Fig. 4. Increased Pax6 level activates *Dbx1* expression in the developing chick pallium. (A) qRT-PCR demonstrates a significant increase in *Dbx1* expression in the E5 chick pallium upon overexpression of Pax6. Error bars indicate s.e.m. $n=3$. Two-tailed Student's *t*-test, *** $P<0.05$. (B) *In situ* hybridization of *Dbx1* mRNA (right) in the E5 chick dorsal (DP) and lateral (LP) pallium electroporated with control or *Pax6* expression vectors. Scale bars: 200 μ m.

(Lu et al., 1996). Because this regulatory region contains sequences that are highly conserved among amniotes (Fig. 5B, Table S2), we isolated corresponding 3.5 kb fragments from both mouse and chick *Dbx1* genomic loci (termed the *Dbx1* 3.5-kb CRM) and examined their Pax6-dependent transcriptional activities. Co-transfection of the Pax6 expression vector and luciferase expression vector containing mouse or chick *Dbx1* 3.5-kb CRM into HEK293T cells significantly increased luciferase activities in a Pax6 dose-dependent manner (Fig. 5C,D). Notably, the chick *Dbx1* 3.5-kb CRM exhibited more pronounced transcriptional activity than the mouse *Dbx1* 3.5-kb CRM for the same amount of Pax6 (Fig. 5D). Transient chromatin immunoprecipitation (ChIP) assays demonstrated significant enrichment of Pax6 at putative Pax6 binding sites (Pax6 BS1-BS7) in the chick *Dbx1* 3.5-kb CRM in HEK293T cells (Fig. S6B,C). Thus, both chick and mouse *Dbx1* 3.5-kb CRMs have conserved transcriptional activities in response to Pax6.

These lines of evidence suggest that the enhancer activity of the CRM that drives *Dbx1* expression in the developing VP is also highly conserved between mouse and chick. To test this, we generated reporter constructs expressing destabilized GFP (dGFP) under the control of either mouse or chick *Dbx1* 3.5-kb CRM, and electroporated these constructs into the developing mouse telencephalon. *pCAG-mRFP* was co-transfected to monitor transfection efficiency. At 24 h after electroporation, we confirmed the induction of dGFP expression by mouse *Dbx1* 3.5-kb CRM in the developing mouse VP, which faithfully recapitulated endogenous *Dbx1* expression in the developing mouse pallium ($n=4$, Fig. 5E). Surprisingly, introduction of the reporter vector with chick *Dbx1* 3.5-kb CRM also induced dGFP expression in the mouse VP ($n=3$, Fig. 5F). Thus, the enhancer activity that drives *Dbx1* expression in the mammalian VP is extensively conserved among amniotes, even though endogenous *Dbx1* expression is not detected in the developing non-mammalian VP.

DISCUSSION

It has been proposed that variable functions of Pax6 and its downstream effectors are crucial in the evolution of the mammalian neocortex (Molnár and Butler, 2002; Aboitiz, 2011; Aboitiz and Zamorano, 2013), although functional conservation and variation of Pax6 have not been empirically addressed. Here, we clarified that Pax6 plays common roles in promoting neuronal differentiation in

the developing chick and mouse telencephalon, whereas stage-specific binary functions of Pax6 are not conserved; in particular, Pax6-dependent maintenance of RGCs in the VZ is unique to mammalian neocortical progenitors at the middle and late embryonic stages (Fig. 6). Interspecies differences in stage-specific neurogenic functions of Pax6 are correlated with temporal regulation of Notch signaling activity. Intriguingly, E11 mouse cortical neural progenitors and E4 and E7 chick pallial neural progenitors exhibited similar responses to functional manipulation of Pax6, including Pax6-dependent negative regulation of Notch signaling. By contrast, Pax6-dependent suppression of Notch signaling was attenuated in E13 and E15 mouse cortical progenitors and E10 chick dorsal pallial progenitors; the former generate later-born cortical neurons, whereas the latter contribute to gliogenesis (Tsai et al., 1981; Cheung et al., 2007). Thus, the mammalian-specific function of Pax6 in the maintenance of RGCs at the later stages of cortical development might be a consequence of the relative shift of the neurogenic period to Pax6-dependent regulatory programs. Time-dependent regulations of the progenitor state by Pax6 are evolutionarily conserved among amniotes, while extension of the neurogenic period provides a mammalian-specific function of Pax6 at the middle and late embryonic stages (Fig. 6). Temporal changes in the Pax6-dependent neurogenic properties of mammalian neural progenitors are linked with the time-dependent regulation of laminar-specific neuron production in the developing mammalian neocortex. Accordingly, the progenitor potential in middle and late corticogenesis is restricted to generating upper cortical neurons that constitute interhemispheric connections, which are thought to be an evolutionary novelty in mammals (Suárez et al., 2014). Thus, it is possible that the Pax6 function in later corticogenesis that maintains progenitor pools was recruited to reserve mammalian-specific fate-committed progenitors during the evolution of mammalian lineages. Consistently, sustained Pax6 expression induced massive production of upper layer cortical neurons derived from Pax6-positive RGCs in the outer SVZ, which underlies the evolutionary expansion of the primate neocortex (Wong et al., 2015).

Several studies have also shown spatiotemporal differences in the neurogenic potential of RGCs in the developing chick pallium (Striedter and Beydler, 1997; Suzuki et al., 2012). Notably, we identified regional differences in the response to high-dose Pax6 between the dorsal and ventral pallium, which are inversely correlated with the medial (dorsal)-low and lateral (ventral)-high neurogenic gradient of the developing chick pallium (Suzuki et al., 2012). Thus, spatially biased neurogenic potentials of chick pallial neural progenitors might constrain the responsiveness to high-dose Pax6. We could not detect obvious differences in the expression level of endogenous Pax6 protein between the dorsal and ventral pallium in chick brain (Fig. 1A), suggesting that additional mechanisms underlie regional differences in progenitor properties.

Interspecies differences in TF binding sites cannot be predicted by genome sequence alignments (Wilson and Odom, 2009). Here, we identified that the chick *Dbx1* 3.5-kb CRM responds to high-dose Pax6 and it retains cryptic enhancer activity to drive reporter gene expression in the developing mouse VP. This provides a novel example in which divergent gene expression is not driven by the simple gain or loss of CRMs. The regulatory mechanisms responsible for the interspecies differences in *Dbx1* expression remain to be elucidated. Induction of *Dbx1* by high-dose Pax6 suggests that the expression level of endogenous Pax6 in the developing chick pallium is below the threshold of *Dbx1* activation; however, we disfavor this possibility because (1) quantitative and

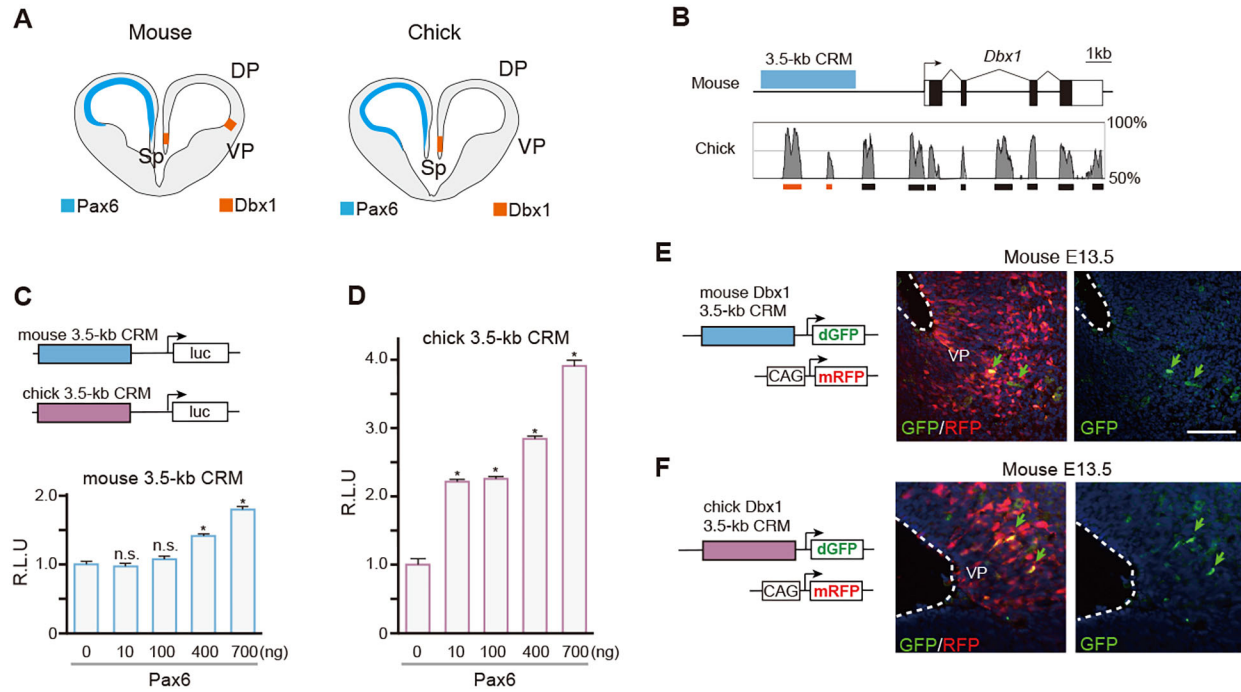


Fig. 5. Evolutionarily conserved enhancer activity of the *Dbx1* 3.5-kb CRM in the developing mouse and chick pallium. (A) Illustration of *Dbx1* and Pax6 expression in the developing mouse and chick telencephalon. Sp, septum. (B) Comparison of the genomic sequences of the mouse and chick *Dbx1* loci. Conserved sequences (boxes at bottom) within the *Dbx1* 3.5-kb CRMs are indicated in orange. (C,D) Luciferase assays with mouse (C) and chick (D) *Dbx1* 3.5-kb CRMs in HEK293T cells. Error bars indicate s.e.m. n=4 for each case. Dunnett's multiple comparison test, *P<0.05. R.L.U, relative luciferase units. (E,F) The expression of destabilized GFP (dGFP) driven by mouse (E) or chick (F) *Dbx1* 3.5-kb CRM in the developing mouse pallium (E13.5). dGFP is specifically expressed in the VP (arrows). Scale bar: 100 μm.

qualitative analyses of *Pax6* transcripts revealed comparable levels in the developing mouse and chick pallium (Fig. 1A; data not shown), (2) our *in vitro* luciferase assay indicated greater transcriptional activity of the chick than mouse *Dbx1* 3.5-kb CRM in the presence of the same amount of Pax6, and (3) the *in vivo* reporter assay demonstrated strong transcriptional activities of mouse and chick *Dbx1* 3.5-kb CRMs in the developing chick pallium (Fig. S7A,B). These results suggest that species-specific differences in *Dbx1* expression might be due to additional suppressive mechanisms mediated by sequence differences in other genomic regions or distinct epigenetic signatures (Fig. 6) (García-Moreno et al., 2018). Several studies have shown that progressive changes in the composition of BAF (Brg1/Brm-associated factor) subunits confer regulation of *Pax6* target genes in the developing mammalian neocortex (Ninkovic et al., 2013; Tuoc et al., 2013; Bachmann et al., 2016). Functional association of these chromatin-remodeling factors with *Pax6* in the developing non-mammalian brain remains to be elucidated.

The extensive conservation of *Pax6*-dependent *Dbx1* regulation suggests that this regulatory mechanism derived from a common ancestor of amniotes (Fig. 6). Although the anatomical structure of ancestral amniote brains remains unknown, it is noteworthy that a part of the genetic program specific for neocortical development is an ancestral character of amniotes. *Pax6*-dependent *Dbx1* expression in the developing spinal cord is highly conserved among vertebrates, and we confirmed that a chick *Dbx1* 3.5-kb CRM has the potential to recapitulate *Dbx1* expression in the developing chick spinal cord (Fig. S7C,D). Thus, one possible scenario is that the gene regulatory mechanisms for the embryonic spinal cord might have been co-opted to recruit *Dbx1* expression in the VP of a common ancestor of amniotes, and further functional

modifications have occurred after the divergence of mammalian and non-mammalian (sauropsid) lineages (Fig. 6). Recent studies indicated that misexpression of *Dbx1* in the developing chick pallium reduced the self-renewal of progenitors while accelerating neurogenesis and inducing reelin expression (Nomura et al., 2008; García-Moreno et al., 2018). Accordingly, we speculate that suppressive mechanisms for *Dbx1* expression in the reptilian and avian VP are prerequisite for sustaining progenitor pools that give rise to the sauropsid-specific dorsal ventricular ridge (Yamashita and Nomura, 2017). It has been proposed that conserved neurogenic programs in ancestral amniotes have been secondarily modified to establish spatially biased neurogenesis in the developing avian pallium (Suzuki and Hirata, 2013). Our results provide mechanistic insight into ancestral neurogenic programs and their functional modifications during amniote brain development and evolution.

MATERIALS AND METHODS

Animals

Fertilized chicken eggs were obtained from a local poultry farm (Yamagishi Farm, Japan) and incubated at 37°C. The stages of the chick embryo were determined according to Hamburger and Hamilton (1951). Pregnant wild-type mice (ICR background, 2–3 months) were purchased from Charles River. Heterozygous *Small eye* (*Sey*) *Pax6* mutant mice (C57BL/6J background) maintained at Tohoku University were intercrossed to obtain homozygous *Sey* embryos. All animal experiments were approved by the Committee of the Kyoto Prefectural University of Medicine (M23-272) and Tohoku University Graduate School of Medicine (#2013-334).

Immunohistochemistry and *in situ* hybridization

Brains were fixed in 4% paraformaldehyde in PBS at 4°C overnight, and then cryoprotected in a 20% sucrose solution and embedded in Tissue-Tek

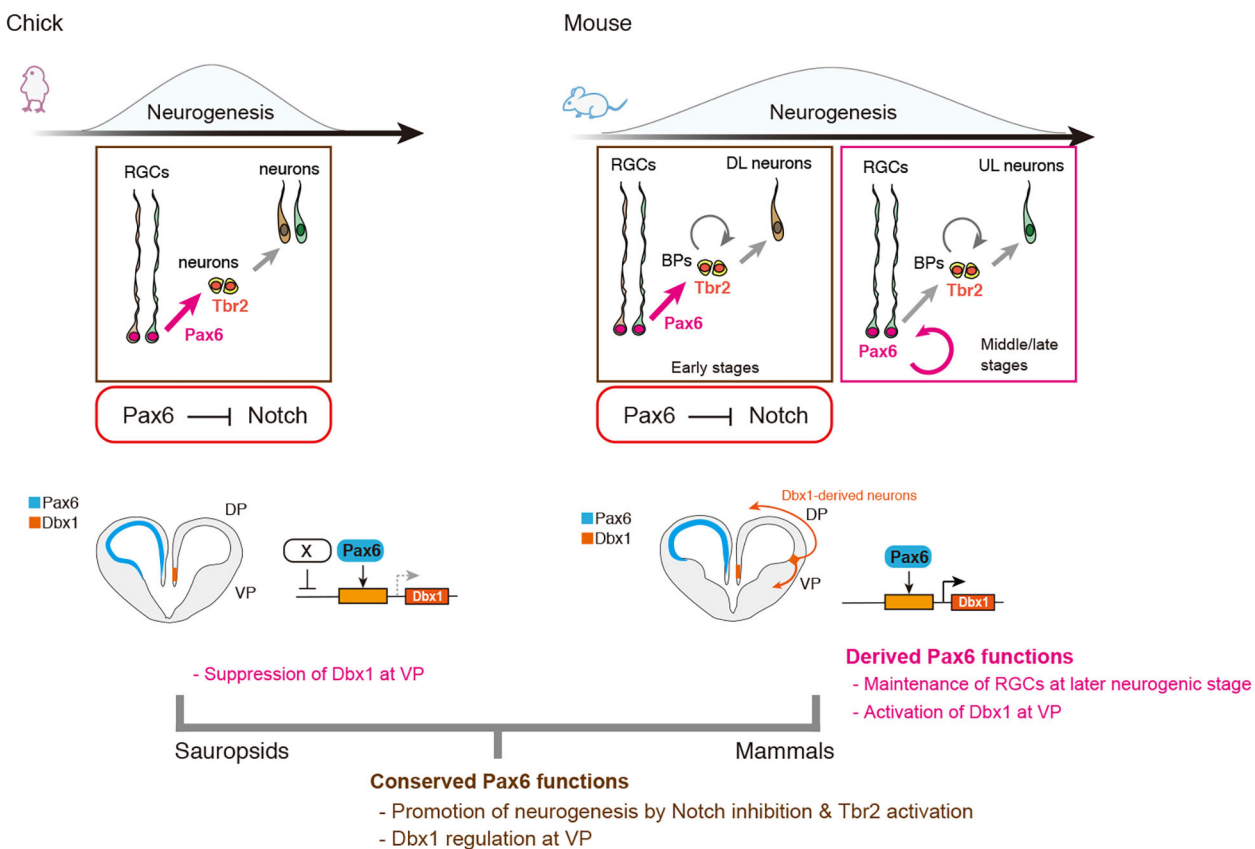


Fig. 6. Conserved and derived functions of Pax6 underlying species-specific neurogenic programs in the developing mouse and chick pallium. (Top) Pax6-dependent suppression of Notch signaling and promotion of neuronal differentiation are highly conserved in developing chick and mouse dorsal pallial progenitors. Conversely, Pax6-dependent maintenance of RGCs at middle/late neurogenic stages is unique to the mouse dorsal pallium (neocortex), which might be a derived Pax6 function in the mammalian lineage. It has also been suggested that fate-restricted RGCs (in different colors) contribute to distinct neuronal subtypes, such as deep (DL) or upper (UL) layer neurons, although our study did not distinguish the heterogeneity of RGCs. Notably, chick ventral pallial progenitors are less sensitive to high doses of Pax6. (Bottom) Structural and functional conservations of *Dbx1* 3.5-kb CRMs suggest that the regulatory mechanism for *Dbx1* expression in the mammalian VP had evolved before the split of mammalian and non-mammalian (sauropsid) lineages. *Dbx1* overexpression is not sufficient to generate tangentially migrating glutamatergic neurons in the developing chick VP (Garcia-Moreno et al., 2018). Thus, in mammals, activation of *Dbx1* expression, as well as additional regulatory networks in the VP, underlie the generation of unique neuronal populations essential for producing mammalian-type pallial structures.

(Sakura). For immunohistochemistry, frozen sections (18 µm) were sliced with a cryostat (CM1850, Leica) and incubated with primary antibodies: anti-Pax6 (rabbit polyclonal, 1:500, PD022, MBL), anti-Gsh2 (rabbit polyclonal, 1:500, ABN162, Merck Millipore), anti-Tbr2 (rabbit polyclonal, 1:500, ab23345, Abcam; rabbit polyclonal, 1:500, HPA028896, Atlas Antibody; chicken polyclonal, 1:500, AB15894, Merck Millipore), anti-Tbr1 (chicken polyclonal, 1:500, AB2261, Merck Millipore), anti-GFP (rabbit polyclonal, 1:500, A11122, Thermo Fisher Scientific; rat monoclonal, 1:500, GF090R 04404-84, Nacalai Tesque), anti-GABA (rabbit monoclonal, 1:500, A2052, Sigma), anti-cleaved caspase 3 (rabbit polyclonal, 1:500, D175, Cell Signaling) and anti-*Dbx1* [rabbit polyclonal, 1:2000, a gift from Dr Shirasaki (Inamata and Shirasaki, 2014)] antibodies. After washing in Tris-buffered saline containing 0.01% Tween 20, the sections were incubated with secondary antibodies: Alexa Fluor 488-, 594- and 633-conjugated anti-rabbit, mouse and rat antibodies (all at 1:500, Thermo Fisher Scientific). Nuclear staining was performed with Hoechst 33258. For Tbr2 staining, heat-mediated antigen retrieval was performed for 20 min at 70°C with HistoVT One (Nacalai Tesque) before incubation with the primary antibody. The sections were analyzed using a fluorescence microscope (BX51, Olympus) equipped with cooled CCD system (DP71, Olympus) and using a laser-scanning confocal microscope (FV1000D, Olympus).

In situ hybridization against chick *Dbx1* was performed as previously described (Nomura et al., 2008). A digoxigenin (DIG)-labeled cRNA probe was synthesized by *in vitro* transcription from chick *Dbx1* cDNA that was subcloned

into the *p3T* vector (Molecular Biotechnology). After the color reaction, images were analyzed using a fluorescence microscope (BX51, Olympus).

***In vivo* genome editing of the chicken Pax6 gene**

Design and validation of CRISPR/Cas9-mediated *in vivo* gene targeting were performed as described (Shimmyo et al., 2016). For plasmid construction, we designed sgRNAs for the chicken *Pax6* gene using CHOPCHOP software (<http://chopchop.cbu.uib.no/>) (Montague et al., 2014), and three sgRNAs targeting the sequences of exon 5, 7 and 8 of *Pax6* were selected and cloned into *pX330-U6-Chimeric_BB-CBh-hSpCas9* (a gift from Feng Zhang, Addgene plasmid #42230; Cong et al., 2013). The primers used for plasmid construction are listed in Table S3. DNA solution (0.1 µl) containing *pX330* (2 µg/µl) and *pCAX-GFP* (0.5 µg/µl) was electroporated into the developing chick pallium. To validate insertions/deletions (indels) of target sequences, the GFP-positive region of the electroporated sample was dissected under a fluorescence microscope (SZX7, Olympus) 36 h after *in ovo* electroporation, and genomic DNA isolated using the DNeasy Blood & Tissue Kit (Qiagen). The target sequence of the sgRNA was amplified by PCR with KOD FX Neo polymerase (TOYOBO) and the following primers: 5'-TGTGGTTCTGTCCGCTTCCT-3' (forward) and 5'-CTGGGGAT-GACCGCGTCGTT-3' (reverse). The PCR amplicons were used for the construction of a library for Illumina sequencing with the KAPA Hyper Prep Kit (Kapa Biosystems) and were sequenced using an Illumina MiSeq sequencer. Indel analysis was performed by mapping the reads to the chick

reference genome sequence (*Gallus gallus* chromosome 5; accession no. NC 006092.4). Under our experimental conditions, it took at least 48 h to detect phenotypes by introduction of sgRNAs; to examine rapid changes in gene expression or cellular dynamics by manipulation of Pax6, we utilized the expression vectors for *Pax6* or *Pax6-EnR*.

In ovo and in utero electroporation

In ovo electroporation of the developing chick and *in utero* electroporation of the developing mouse neocortex were performed as described (Nomura et al., 2013). Briefly, ~0.1 µl DNA solution was injected into the lateral ventricle of each embryo using a glass needle. Then, needle-type electrodes (CUY200S, BEX) were placed on the embryo head, and square electric pulses (28–32V, 50 ms, 3–4 times) were applied with a pulse generator (CUY21 EDITII, BEX). Electroporated chick embryos were placed in incubators at 37°C. To prepare the DNA solution, various expression vectors, including *pCAX-GFP*, *pX330-gRNAs*, *pCAX-Pax6*, *pMIWIII-Pax6-EnR*, were dissolved at 0.5–2.5 µg/µl in PBS containing 0.05% Fast Green.

Clonal analysis

For clonal analysis of chick neural progenitors, *Cytbow* and *Nucbow* vectors, self-excision Cre expression vector (*pSE-Cre*) and a transposase expression vector (*pBase*) were mixed with a *pCAG* empty vector or *pCAX-Pax6*, as previously reported (Loulier et al., 2014), and electroporated into the E4 chick dorsal pallium. Fluorescent images of brain sections were captured by a laser-scanning confocal microscope (FV1000). Labeled cells with the same combination of fluorescent proteins in side-by-side serial sections were regarded as clonal siblings. We chose rare combinations of fluorescent proteins to avoid misinterpreting the clonal relationships of labeled cells.

Quantitative real-time PCR (qRT-PCR)

After electroporation of *pCAX-Pax6* and/or *pCAX-GFP*, the GFP-positive chick pallial region was manually dissected under the fluorescence microscope, and total RNA was extracted using the RNeasy Mini Kit (Qiagen), and cDNA was synthesized using random primers with reverse transcriptase (ReverTra Ace, TOYOBO). qPCR was performed on a Light Cycler Nano (Roche) with THUNDERBIRD SYBR qPCR Mix (TOYOBO) according to the manufacturers' protocols. Gene expression levels were normalized to those of amplification of β-actin. Primer sequences for qPCR (Table S3) were designed by primer-BLAST (NCBI). qPCR was carried out on three independent samples with two technical replicates.

Labeling of S-phase cells

To detect cells undergoing S-phase, 5-ethynyl-2'-deoxyuridine (EdU; 10 mg/ml, Thermo Fisher Scientific) was injected into the lateral ventricle in developing chick embryos (0.1 µl) and the peritoneum in pregnant mice (100 mg/kg) 1 h before fixation. EdU detection was with the Click-iT Plus Kit (Thermo Fisher Scientific).

Luciferase reporter assay

To quantify the activity of Notch signaling, the vectors *p4xCSL-firefly luciferase* (Addgene #41726), *pRL-SV40* (Promega) and *pCAX-GFP* were co-electroporated into the dissociated neural progenitors using electroporation cuvettes (SE-202, BEX). After electroporation, neural progenitors were cultured as floating cell aggregates for 24 h in Neurobasal medium supplemented with GlutaMAX, B27 supplement (Thermo Fisher Scientific) and FGF2 (10 ng/ml), as previously reported (Yamashita et al., 2017). To examine the transcriptional activity of mouse and chicken *Dbx1* 3.5-kb CRMs, HEK293T cells (RIKEN BRC; contamination has been checked routinely) were transfected with *pGL3-promoter* vectors (Promega) containing mouse or chicken *Dbx1* 3.5-kb CRM together with *pRL-SV40* and *pCAX-mouse Pax6* vectors using Lipofectamine 2000 (Thermo Fisher Scientific). Luciferase reporter activity was examined with the Dual-Luciferase Reporter Assay System (Promega). Chemical luminescence was analyzed with a luminometer (GENE LIGHT GL210A, Microtec). All firefly luciferase values were normalized to *Renilla* luciferase activities to quantify relative luciferase units. Each experiment was carried out in four biological replicates.

RNA-seq data analysis

After electroporation of *pCAX-Pax6* and/or *pCAX-GFP*, GFP-positive chick pallial regions were manually dissected under a fluorescence microscope. Total RNA was extracted from dissected tissues with the RNeasy Plus Universal Kit (Qiagen) according to the manufacturer's instructions. RNA quality was assessed using a NanoDrop 1000 spectrophotometer (Thermo Fisher Scientific) and an Agilent 2100 Bioanalyzer (Agilent Laboratories). The cDNA library was constructed using the TruSeq Stranded Total RNA Library Prep Kit (Illumina) and paired-end sequencing was performed with a HiSeq 2500 (Illumina). Sequencing data were mapped to a reference genome sequence (Galgal4; retrieved from the Ensembl genome browser database) and quantified by differential gene expression analyses.

Isolation of mouse and chicken *Dbx1* 3.5-kb CRMs

The mouse *Dbx1* 3.5-kb CRM located 2.7 kb upstream of the transcription start site was isolated from C3H mouse genomic DNA and cloned into *pGL3-promoter* (Promega) and *pTAL-d2GFP* (Clontech) vectors. The chicken *Dbx1* 3.5-kb CRM was isolated from a BAC clone (CH261-63F7, BAC PAC Resources) based on chicken genomic information (*Gallus gallus*-5.0). The primer sequences for PCR amplification of mouse and chick *Dbx1* 3.5-kb CRM are listed in Table S2.

Chromatin immunoprecipitation assay

The transient ChIP assay was performed as previously described (Lavarrar and Farnham, 2004). Briefly, HEK293T cells were transfected with *pCAG-chick Pax6* and *pGL3-chick Dbx1* 3.5-kb CRM using Lipofectamine 2000. At 24 h after transfection, cells were cross-linked with formaldehyde for 10 min and then harvested to isolate nuclear extracts. ChIP was carried out with the Simple ChIP Plus Kit (Cell Signaling Technology) according to the manufacturer's protocol. Anti-Pax6 antibody (MBL, 1:100), anti-IgG and anti-Histone H3 antibodies (Cell Signaling Technology, 1:250 and 1:50, respectively) were used for immunoprecipitation. Genomic fragments containing putative Pax6 binding sites (BS1-2, BS3-4, BS5-6, and BS7) in the chick *Dbx1* 3.5-kb CRM were amplified by qPCR with specific primers (Table S2).

Quantification and statistical analyses

Cell numbers were quantified by image capture with a laser-scanning confocal microscope (FV1000D, Olympus) and analysis with ImageJ (NIH) software. Three representative sections of each sample were selected for cell counting. All quantitative data were obtained from six samples and are presented as mean±s.e.m. The variances of each data point were checked by *F*-test, and the statistical significance of mean values was calculated using two-tailed Student's *t*-test, Welch's *t*-test or Dunnett's multiple comparison test.

Acknowledgements

We thank Ms Misato Kawami, Sayaka Makino and Mr Toyo Shimizu for technical assistance, Dr Ryuichi Shirasaki for providing anti-*Dbx1* antibody, Drs Jean Livet and Josh Breunig for providing the *Nucbow* and *Cytbow* vectors, Dr Fernando Garcia-Moreno for sharing unpublished data, and Dr Ikuo K. Suzuki for critical comments on the manuscript.

Competing interests

The authors declare no competing or financial interests.

Author contributions

Conceptualization: W.Y., K.O., T.N.; Methodology: W.Y., M.T., H.G., T.N.; Validation: W.Y., M.T., T.K., T.N.; Formal analysis: W.Y., T.N.; Investigation: W.Y., M.T., T.K., H.G., T.N.; Resources: W.Y., M.T., T.K., H.G., N.O., K.O., T.N.; Data curation: W.Y., T.N.; Writing - original draft: W.Y., T.N.; Writing - review & editing: W.Y., M.T., T.K., H.G., N.O., K.O., T.N.; Visualization: W.Y., T.N.; Supervision: K.O.; Project administration: T.N.; Funding acquisition: W.Y., N.O., T.N.

Funding

This work was supported by a Japan Society for the Promotion of Science (JSPS) Research Fellowship for Young Scientists (16J09444) to W.Y.; JSPS KAKENHI [16H01324 (Thermal Biology), 17H03552] to T.N.; Japan Science and Technology Agency (JST) PRESTO (Design and Control of Cellar Functions: JPMJPR12AA) to T.N.; Yamada Science Foundation (29-007) to T.N.; and JSPS KAKENHI [16H06530] to N.O. Deposited in PMC for immediate release.

Data availability

RNA-seq data have been deposited at the DNA Data Bank of Japan (DDBJ) Sequence Read Archive under accession numbers DRA005904 and DRA006015. Raw data (datasets used to produce figures) have been deposited at Figshare: Pax6 functions in development and evolution of amniote brains (<https://doi.org/10.6084/m9.figshare.5873703.v2>).

Supplementary information

Supplementary information available online at <http://dev.biologists.org/lookup/doi/10.1242/dev.159764.supplemental>

References

- Aboitiz, F. (2011). Genetic and developmental homology in amniote brains. Toward conciliating radical views of brain evolution. *Brain Res. Bull.* **84**, 125-136.
- Aboitiz, F. and Zamorano, F. (2013). Neural progenitors, patterning and ecology in neocortical origins. *Front. Neuroanat.* **7**, 38.
- Assimacopoulos, S., Grove, E. A. and Ragsdale, C. W. (2003). Identification of a Pax6-dependent epidermal growth factor family signaling source at the lateral edge of the embryonic cerebral cortex. *J. Neurosci.* **23**, 6399-6403.
- Bachmann, C., Nguyen, H., Rosenbusch, J., Pham, L., Rabe, T., Patwa, M., Sokpor, G., Seong, R. H., Ashery-Padan, R., Mansouri, A. et al. (2016). mSWI/ SNF (BAF) complexes are indispensable for the neurogenesis and development of embryonic olfactory epithelium. *PLoS Genet.* **12**, e1006274.
- Bielle, F., Griveau, A., Narboux-Nême, N., Vigneau, S., Sigrist, M., Arber, S., Wassef, M. and Pierani, A. (2005). Multiple origins of Cajal-Retzius cells at the borders of the developing pallium. *Nat. Neurosci.* **8**, 1002-1012.
- Carney, R. S., Cucas, L. A., Hirata, T., Mansfield, K. and Corbin, J. G. (2009). Differential regulation of telencephalic pallial-subpallial boundary patterning by Pax6 and Gsh2. *Cereb. Cortex* **19**, 745-759.
- Carroll, S. B. (2005). Evolution at two levels: on genes and form. *PLoS Biol.* **3**, e245.
- Cheung, A. F., Pollen, A. A., Tavare, A., DeProto, J. and Molnár, Z. (2007). Comparative aspects of cortical neurogenesis in vertebrates. *J. Anat.* **211**, 164-176.
- Cong, L., Ran, F. A., Cox, D., Lin, S., Barretto, R., Habib, N., Hsu, P. D., Wu, X., Jianh, W., Marraffini, L. A. et al. (2013). Multiplex genome engineering using CRISPR/Cas systems. *Science* **339**, 819-823.
- Duparc, R.-H., Abdouh, M., David, J., Lépine, M., Tétreault, N. and Bernier, G. (2007). Pax6 controls the proliferation rate of neuroepithelial progenitors from the mouse optic vesicle. *Dev. Biol.* **301**, 374-387.
- Estivill-Torrus, G., Pearson, H., Heyning, V. V., Price, D. J. and Rashbass, P. (2002). Pax6 is required to regulate the cell cycle and the rate of progression from symmetrical to asymmetrical division in mammalian cortical progenitors. *Development* **129**, 455-466.
- Fernandez, A. S., Pieau, C., Reperant, J., Boncinelli, E. and Wassef, M. (1998). Expression of the Emx-1 and Dlx-1 homeobox genes define three molecularly distinct domains in the telencephalon of mouse, chick, turtle and frog embryos: implications for the evolution of telencephalic subdivisions in amniotes. *Development* **125**, 2099-2111.
- Fukuda, T., Kawano, H., Osumi, N., Eto, K. and Kawamura, K. (2000). Histogenesis of the cerebral cortex in rat fetuses with a mutation in the Pax-6 gene. *Brain Res. Dev. Brain Res.* **120**, 65-75.
- García-Moreno, F. and Molnár, Z. (2015). Subset of early radial glial progenitors that contribute to the development of callosal neurons is absent from avian brain. *Proc. Natl. Acad. Sci. USA* **112**, E5058-E5067.
- García-Moreno, F., Anderton, E., Jankowska, M., Begbie, J., Encinas, J. M., Irimia, M. and Molnár, Z. (2018). Absence of tangentially migrating glutamatergic neurons in the developing avian brain. *Cell Rep.* **22**, 96-109.
- Glassford, W. J., Johnson, W. C., Dall, N. R., Smith, S. J., Liu, Y., Boll, W., Noll, M. and Rebeiz, M. (2015). Co-option of an ancestral Hox-regulated network underlies a recently evolved morphological novelty. *Dev. Cell* **34**, 520-531.
- Götz, M. and Huttner, W. B. (2005). The cell biology of neurogenesis. *Nat. Rev. Mol. Cell Biol.* **6**, 777-788.
- Hamburger, V. and Hamilton, H. L. (1951). A series of normal stages in the development of the chick embryo. *J. Morphol.* **88**, 49-92.
- Heffer, A., Shultz, J. W. and Pick, L. (2010). Surprising flexibility in a conserved Hox transcription factor over 550 million years of evolution. *Proc. Natl. Acad. Sci. USA* **107**, 18040-18045.
- Hirata, T., Li, P., Lanuza, G. M., Cucas, L. A., Huntsman, M. M. and Corbin, J. G. (2009). Identification of distinct telencephalic progenitor pools for neuronal diversity in the amygdala. *Nat. Neurosci.* **12**, 141-149.
- Holm, P. C., Mader, M. T., Haubst, N., Wizenmann, A., Sigvardsson, M. and Götz, M. (2007). Loss- and gain-of-function analyses reveal targets of Pax6 in the developing mouse telencephalon. *Mol. Cell. Neurosci.* **34**, 99-119.
- Inamata, Y. and Shirasaki, R. (2014). Dbx1 triggers crucial molecular programs required for midline crossing by midbrain commissural axons. *Development* **141**, 1260-1271.
- Kriegstein, A., Noctor, S. and Martínez-Cerdeño, V. (2006). Patterns of neural stem and progenitor cell division may underlie evolutionary cortical expansion. *Nat. Rev. Neurosci.* **7**, 883-890.
- Kroll, T. T. and O'Leary, D. D. M. (2005). Ventralized dorsal telencephalic progenitors in Pax6 mutant mice generate GABA interneurons of a lateral ganglionic eminence fate. *Proc. Natl. Acad. Sci. USA* **102**, 7374-7379.
- Kvon, E. Z., Kamneva, O. K., Melo, U. S., Barozzi, I., Osterwalder, M., Mannion, B. J., Tissieres, V., Pickle, C. S., Plajzer-Frick, I., Lee, E. A. et al. (2016). Progressive loss of function in a limb enhancer during snake evolution. *Cell* **167**, 633-642.e611.
- Lavrkar, J. L. and Farnham, P. J. (2004). The use of transient chromatin immunoprecipitation assays to test models for E2F1-specific transcriptional activation. *J. Biol. Chem.* **279**, 46343-46349.
- Loulier, K., Barry, R., Mahou, P., Le Franc, Y., Supatto, W., Matho, K. S., Ieng, S., Fouquet, S., Dupin, E., Benosman, R. et al. (2014). Multiplex cell and lineage tracking with combinatorial labels. *Neuron* **81**, 505-520.
- Lu, S., Shashikant, C. S. and Ruddle, F. H. (1996). Separate cis-acting elements determine the expression of mouse Dbx gene in multiple spatial domains of the central nervous system. *Mech. Dev.* **58**, 193-202.
- Manuel, M. N., Mi, D., Mason, J. O. and Price, D. J. (2015). Regulation of cerebral cortical neurogenesis by the Pax6 transcription factor. *Front. Cell Neurosci.* **9**, 70.
- Medina, L. and Reiner, A. (2000). Do birds possess homologues of mammalian primary visual, somatosensory and motor cortices? *Trends Neurosci.* **23**, 1-12.
- Molnár, Z. and Butler, A. B. (2002). The corticostratal junction: a crucial region for forebrain development and evolution. *BioEssays* **24**, 530-541.
- Montague, T. G., Cruz, J. M., Gagnon, J. A., Church, G. M. and Valen, E. (2014). CHOPCHOP: a CRISPR/Cas9 and TALEN web tool for genome editing. *Nucleic Acids Res.* **42**, W401-W407.
- Nieuwenhuys, R. (1994). The neocortex. An overview of its evolutionary development, structural organization and synaptology. *Anat. Embryol. (Berl)* **190**, 307-337.
- Ninkovic, J., Steiner-Mezzadri, A., Jawerka, M., Akinci, U., Masserdotti, G., Petricca, S., Fischer, J., von Holst, A., Beckers, J., Lie, C. D. et al. (2013). The BAF complex interacts with Pax6 in adult neural progenitors to establish a neurogenic cross-regulatory transcriptional network. *Cell Stem Cell* **13**, 403-418.
- Nomura, T., Holmberg, J., Frisen, J. and Osumi, N. (2006). Pax6-dependent boundary defines alignment of migrating olfactory cortex neurons via the repulsive activity of ephrin A5. *Development* **133**, 1335-1345.
- Nomura, T., Takahashi, M., Hara, Y. and Osumi, N. (2008). Patterns of neurogenesis and amplitude of Reelin expression are essential for making a mammalian-type cortex. *PLoS ONE* **3**, e1454.
- Nomura, T., Gotoh, H. and Ono, K. (2013). Changes in the regulation of cortical neurogenesis contribute to encephalization during amniote brain evolution. *Nat. Commun.* **4**, 2206.
- Nomura, T., Ohtaka-Maruyama, C., Yamashita, W., Wakamatsu, Y., Murakami, Y., Calegari, F., Suzuki, K., Gotoh, H. and Ono, K. (2016). The evolution of basal progenitors in the developing non-mammalian brain. *Development* **143**, 66-74.
- Numayama-Tsuruta, K., Arai, Y., Takahashi, M., Sasaki-Hoshino, M., Funatsu, N., Nakamura, S. and Osumi, N. (2010). Downstream genes of Pax6 revealed by comprehensive transcriptome profiling in the developing rat hindbrain. *BMC Dev. Biol.* **10**, 6.
- Osumi, N., Shinohara, H., Numayama-Tsuruta, K. and Maekawa, M. (2008). Concise review: Pax6 transcription factor contributes to both embryonic and adult neurogenesis as a multifunctional regulator. *Stern Cells* **26**, 1663-1672.
- Peter, I. S. and Davidson, E. H. (2011). Evolution of gene regulatory networks controlling body plan development. *Cell* **144**, 970-985.
- Puelles, L., Kuwana, E., Puelles, E., Bulfone, A., Shimamura, K., Keleher, J., Smiga, S. and Rubenstein, J. L. R. (2000). Pallial and subpallial derivatives in the embryonic chick and mouse telencephalon, traced by the expression of the genes Dlx-2, Emx-1, Nkx-2.1, Pax-6, and Tbr-1. *J. Comp. Neurol.* **424**, 409-438.
- Puelles, L., Medina, L., Borello, U., Legaz, I., Teissier, A., Pierani, A. and Rubenstein, J. L. R. (2016). Radial derivatives of the mouse ventral pallium traced with Dbx1-LacZ reporters. *J. Chem. Neuroanat.* **75**, 2-19.
- Sansom, S. N., Griffiths, D. S., Faedo, A., Kleinjan, D.-J., Ruan, Y., Smith, J., van Heyningen, V., Rubenstein, J. L. and Livesey, F. J. (2009). The level of the transcription factor Pax6 is essential for controlling the balance between neural stem cell self-renewal and neurogenesis. *PLoS Genet.* **5**, e1000511.
- Schmidt, D., Wilson, M. D., Ballester, B., Schwalie, P. C., Brown, G. D., Marshall, A., Kutter, C., Watt, S., Martinez-Jimenez, C. P., Mackay, S. et al. (2010). Five-vertebrate ChIP-seq reveals the evolutionary dynamics of transcription factor binding. *Science* **328**, 1036-1040.
- Shinmyo, Y., Tanaka, S., Tsunoda, S., Hosomichi, K., Tajima, A. and Kawasaki, H. (2016). CRISPR/Cas9-mediated gene knockout in the mouse brain using in utero electroporation. *Sci. Rep.* **6**, 20611.
- Striedter, G. F. (2005). *Principles of Brain Evolution*. Sunderland, MA: Sinauer.
- Striedter, G. F. and Beydler, S. (1997). Distribution of radial glia in the developing telencephalon of chicks. *J. Comp. Neurol.* **387**, 399-420.
- Suárez, R., Gobius, I. and Richards, L. J. (2014). Evolution and development of interhemispheric connections in the vertebrate forebrain. *Front. Hum. Neurosci.* **8**, 497.
- Sugahara, F., Pascual-Anaya, J., Oisi, Y., Kuraku, S., Aota, S., Adachi, N., Takagi, W., Hirai, T., Sato, N., Murakami, Y. et al. (2016). Evidence from cyclostomes for complex regionalization of the ancestral vertebrate brain. *Nature* **531**, 97-100.

- Suzuki, I. K. and Hirata, T.** (2013). Neocortical neurogenesis is not really "neo": a new evolutionary model derived from a comparative study of chick pallial development. *Dev. Growth Differ.* **55**, 173-187.
- Suzuki, I. K., Kawasaki, T., Gojobori, T. and Hirata, T.** (2012). The temporal sequence of the mammalian neocortical neurogenetic program drives mediolateral pattern in the chick pallium. *Dev. Cell* **22**, 863-870.
- Takahashi, M. and Osumi, N.** (2002). Pax6 regulates specification of ventral neurone subtypes in the hindbrain by establishing progenitor domains. *Development* **129**, 1327-1338.
- Teissier, A., Griveau, A., Vigier, L., Piolot, T., Borello, U. and Pierani, A.** (2010). A novel transient glutamatergic population migrating from the pallial-subpallial boundary contributes to neocortical development. *J. Neurosci.* **30**, 10563-10574.
- Thakurela, S., Tiwari, N., Schick, S., Garding, A., Ivanek, R., Berninger, B. and Tiwari, V. K.** (2016). Mapping gene regulatory circuitry of Pax6 during neurogenesis. *Cell Discov.* **2**, 15045.
- Toresson, H., Potter, S. S. and Campbell, K.** (2000). Genetic control of dorsal-ventral identity in the telencephalon: opposing roles for Pax6 and Gsh2. *Development* **127**, 4361-4371.
- Tsai, H. M., Garber, B. B. and Laramendi, L. M.** (1981). 3H-thymidine autoradiographic analysis of telencephalic histogenesis in the chick embryo: I. Neuronal birthdates of telencephalic compartments in situ. *J. Comp. Neurol.* **198**, 275-292.
- Tuoc, T. C., Radyushkin, K., Tonchev, A. B., Pinon, M. C., Ashery-Padan, R., Molnár, Z., Davidoff, M. S. and Stoykova, A.** (2009). Selective cortical layering abnormalities and behavioral deficits in cortex-specific Pax6 knock-out mice. *J. Neurosci.* **29**, 8335-8349.
- Tuoc, T. C., Boretius, S., Sansom, S. N., Pitulescu, M.-E., Frahm, J., Livesey, F. J. and Stoykova, A.** (2013). Chromatin regulation by BAF170 controls cerebral cortical size and thickness. *Dev. Cell* **25**, 256-269.
- Ulinski, P. S.** (1983). *Dorsal Ventricular Ridge: Treatise on Forebrain Organization in Reptiles and Birds (Neurobiology)*. John Wiley & Sons.
- Ulinski, P. S.** (1990). The cerebral cortex of reptiles. In *Comparative Structure and Evolution of Cerebral Cortex, Part I* (ed. E. G. Jones and A. Peters), pp. 139-215. New York: Plenum.
- Wagner, G. P.** (2007). The developmental genetics of homology. *Nat. Rev. Genet.* **8**, 473-479.
- Wilson, M. D. and Odom, D. T.** (2009). Evolution of transcriptional control in mammals. *Curr. Opin. Genet. Dev.* **19**, 579-585.
- Wong, F. K., Fei, J.-F., Mora-Bermúdez, F., Taverna, E., Haffner, C., Fu, J., Anastassiadis, K., Stewart, A. F. and Huttner, W. B.** (2015). Sustained Pax6 expression generates primate-like basal radial glia in developing mouse neocortex. *PLoS Biol.* **13**, e1002217.
- Yamashita, W. and Nomura, T.** (2017). The neocortex and dorsal ventricular ridge: functional convergence and underlying developmental mechanisms. In *Brain Evolution by Design - From Neural Origin to Cognitive Architecture* (ed. S. Shigeno, Y. Murakami and T. Nomura), pp. 291-310. Tokyo: Springer.
- Yamashita, W., Shimizu, T. and Nomura, T.** (2017). In vitro and ex ovo culture of reptilian and avian neural progenitor cells. *Methods Mol. Biol.* **1650**, 259-265.
- Ypsilanti, A. R. and Rubenstein, J. L. R.** (2016). Transcriptional and epigenetic mechanisms of early cortical development: An examination of how Pax6 coordinates cortical development. *J. Comp. Neurol.* **524**, 609-629.
- Yun, K., Potter, S. and Rubenstein, J. L.** (2001). Gsh2 and Pax6 play complementary roles in dorsoventral patterning of the mammalian telencephalon. *Development* **128**, 193-205.
- Zhang, X., Huang, C. T., Chen, J., Pankratz, M. T., Xi, J., Li, J., Yang, Y., Lavaute, T. M., Li, X.-J., Ayala, M. et al.** (2010). Pax6 is a human neuroectoderm cell fate determinant. *Cell Stem Cell* **7**, 90-100.

Supplementary Information

A

Target PAM

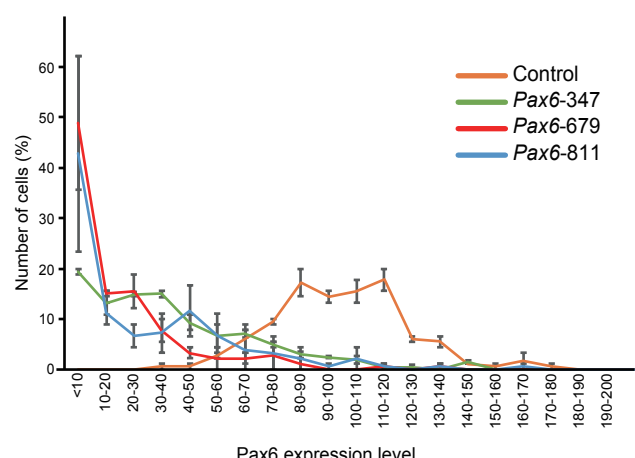
Pax6-347 5' -CACAGCGGCGTGAACCAGCTCGGCCGGGTGTTG- 3'
Pax6-679 5' -GATTGAGACAGATTACTCTCGGAGGGGTCTG- 3'
Pax6-811 5' -GCTAAGGATGCTGAACGGGCAGACGGGACATG- 3'

B

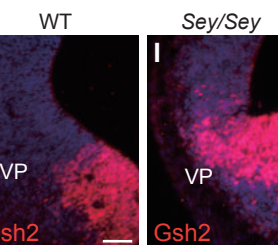
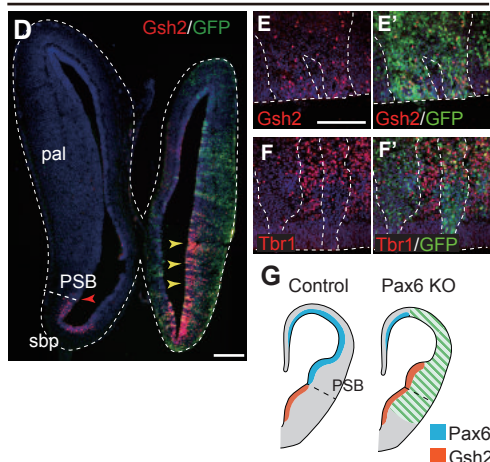
Wild-Type 5' -GATTGAGACAGATTACTC-TCGGAGGGGTCTG- 3' (0)

1	5' -GATTGAG-----ACAGAGGGGTCTG- 3' (-11)
2	5' -----3' (-112)
3	5' -GATTGAGACAGATTACTC--TCGAGGGGTCTG- 3' (-1)
4	5' -----3' (-146)
5	5' -----GGGGTCTG- 3' (-50)
6	5' -GATTGAGACAGATTACTCTCGGAGGGGTCTG- 3' (+1)

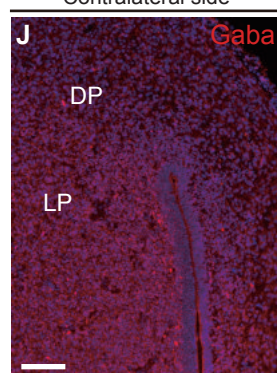
C



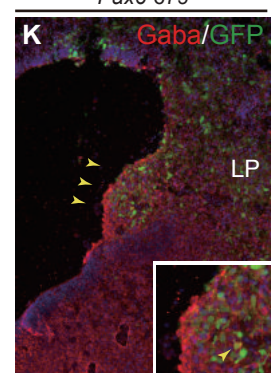
D Pax6-679



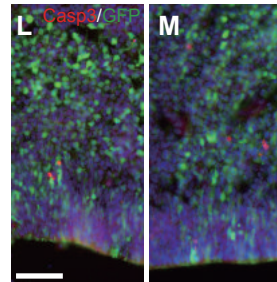
J



K



L



M

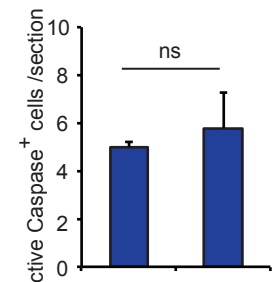


Fig. S1 (related to Fig. 1). CRISPR/Cas9-mediated targeting of the *Pax6* gene in the developing chick pallium.

(A) Target sequences of single-guide RNAs (sgRNA) (green) upstream of the PAM sequence (red) in the chick *Pax6* gene. (B) Representative mutant sequences of Pax6 after electroporation of *pX330-Pax6-679*. Indels are indicated in blue. Target sequences of sgRNA and PAM sequences are indicated as green and red, respectively. (C) The expression level of Pax6 in the developing chick pallium after electroporation of *pX330-Pax6* vectors. The histogram shows the signal intensity of Pax6 in samples transfected with control vector or *pX330-Pax6* vectors (mean ± s.e., n=4 animals in each group). (D, E, E', F, F') Ectopic expression of Gsh2 and reduced Tbr1 expression in the E6 chick pallium transfected with *pX330-Pax6-679*. (G) Schematic illustration of the phenotype of the *Pax6*-deleted chick pallium. The area shown with a green oblique line indicates the electroporated region. (H, I) Gsh2 expression in E12.5 wild-type (H) and *Small eye (Sey/Sey)* (I) mice. In *Sey/Sey*, ectopic Gsh2 expression is evident at the VP. (J, K) Accumulation of Gaba-positive cells in the ventricular zone of E10 chick pallium transfected with *pX330-Pax6-679*. (L-N) Active caspase 3-positive cells in brains transfected with control and *pX330-Pax6-679* vectors. Scale bars: 200 µm (D, H, J), 50 µm (E, L).

Chick E4- E5 Clonal Analyses

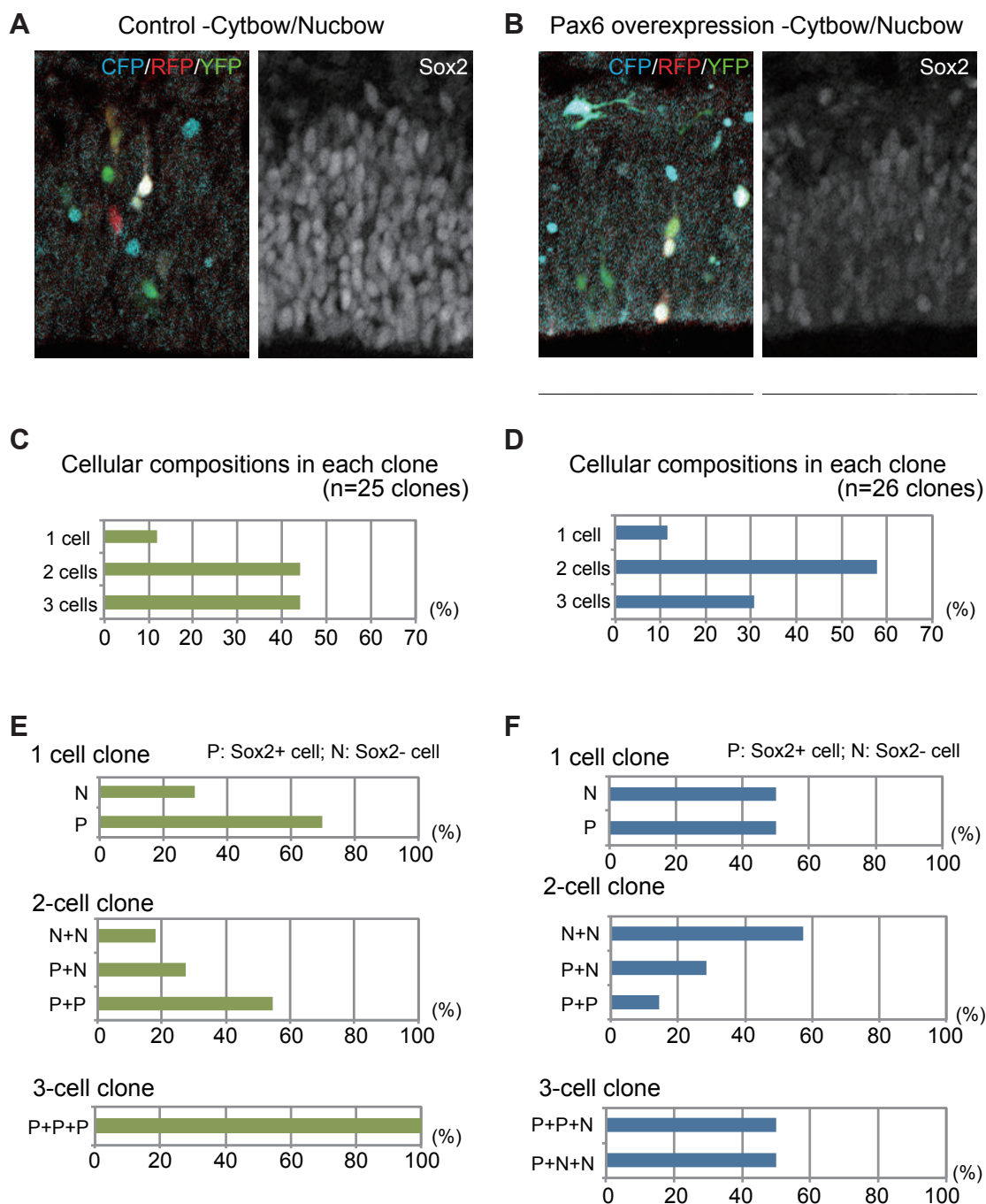


Fig. S2 (related to Fig. 2). High-dose Pax6 increases neurogenic divisions in the developing chick pallium.

(A, B) Distributions of clonally related cells in E5 chick pallium transfected with control and *Pax6* expression vectors. Clonal siblings are labeled by co-electroporation of *Cytobow/Nucbow* and the self-excision Cre expression vector. (C-F) Cell compositions in each clone in control (C, E) and *Pax6*-overexpressed brains (D, F). Progenitors (P) and non-progenitors (N) are distinguished by Sox2 expression. High-dose *Pax6* decreases the proportion of progenitors and increases non-progenitors in individual clones. n=2 brains for each case.

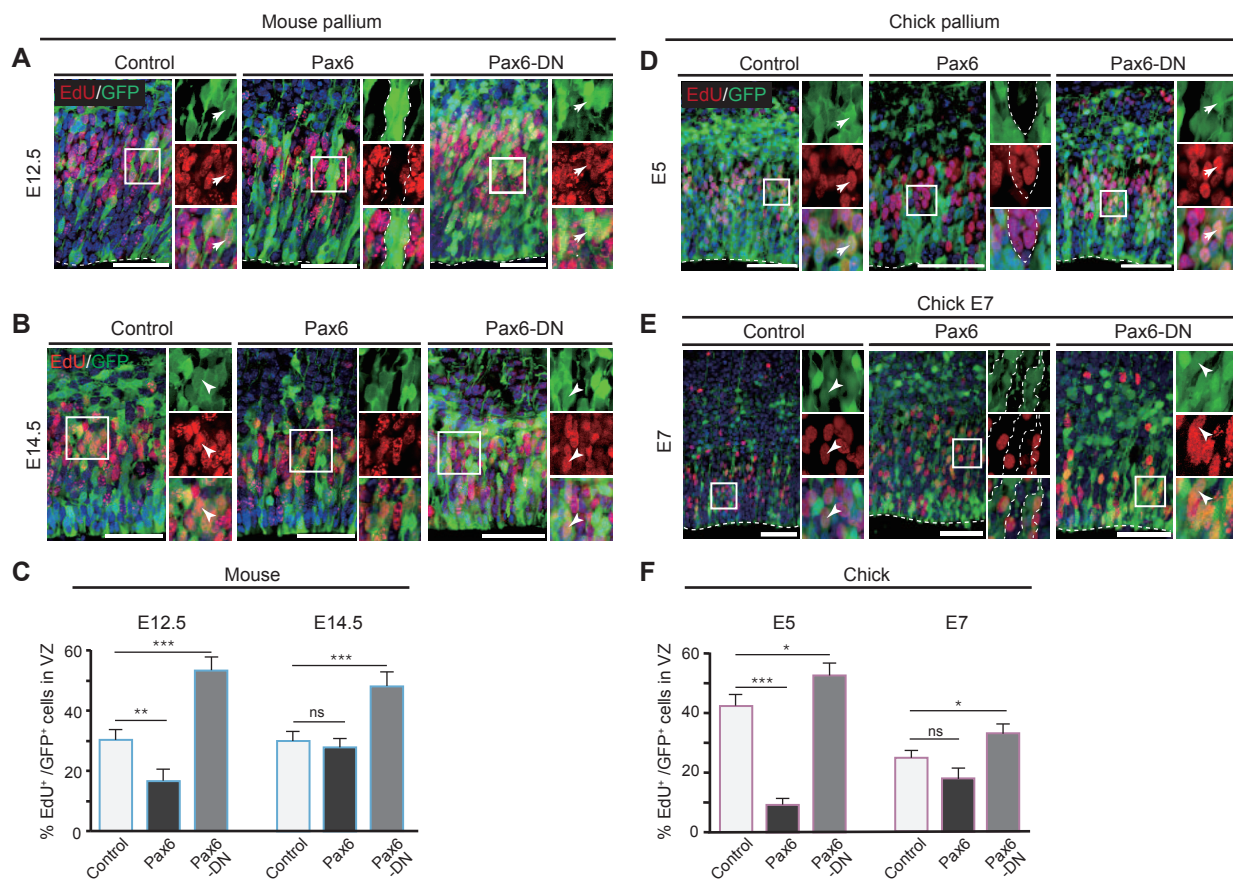


Fig. S3 (related to Fig. 2). Pax6-dependent negative regulation of progenitor proliferation in the developing mouse and chick dorsal pallium.

(A, B, D, E) EdU-positive cells in the E12.5 (A) and E14.5 (B) mouse and E5 (D) and E7 (E) chick dorsal pallium after electroporation of control (GFP), *Pax6* or *Pax6-DN* vectors. Insets show representative EdU-positive cells in GFP⁺ transfected cells (white arrowheads). (C, F) The proportion of EdU-positive cells in GFP-positive cells in the VZ of mouse (C) and chick (F) dorsal pallium. Data indicate the mean ± s.e., n=6 for each case, Student's t-test, *P < 0.05, **P < 0.01, ***P < 0.005. Scale bars: 50 μm.

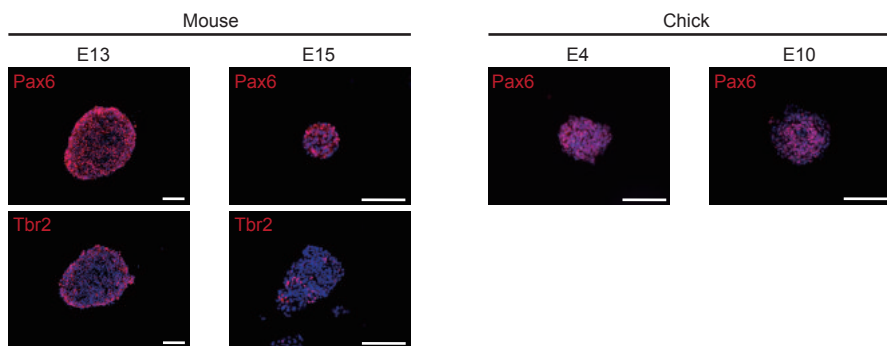


Fig. S4 (related to Fig. 3). Pax6 and Tbr2 expression in mouse and chick neurospheres.

Immunohistochemistry of neurospheres derived from the E13 or E15 mouse neocortex and the E4 or E10 chick pallium with anti-Pax6 or –Tbr2 antibodies. Scale bar: 100 μ m.

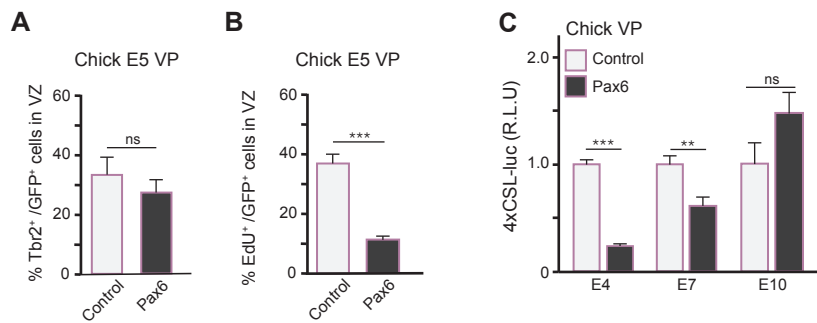


Fig. S5 (related to Fig. 3). Pax6 gain-of-function analysis of chick ventral pallial progenitors.

(A, B) Tbr2- and EdU-positive cells in the E5 chick ventral pallium after electroporation of control (GFP) or Pax6 vectors. (C) Pax6-dependent changes in Notch reporter (*p4xCSL*-luciferase) activity in neuronal progenitors from the E4, E7 or E10 chick ventral pallium. Data indicate the represented mean \pm s.e., at least n=3 for each case, Student's *t*-test, *P < 0.05, **P < 0.01.

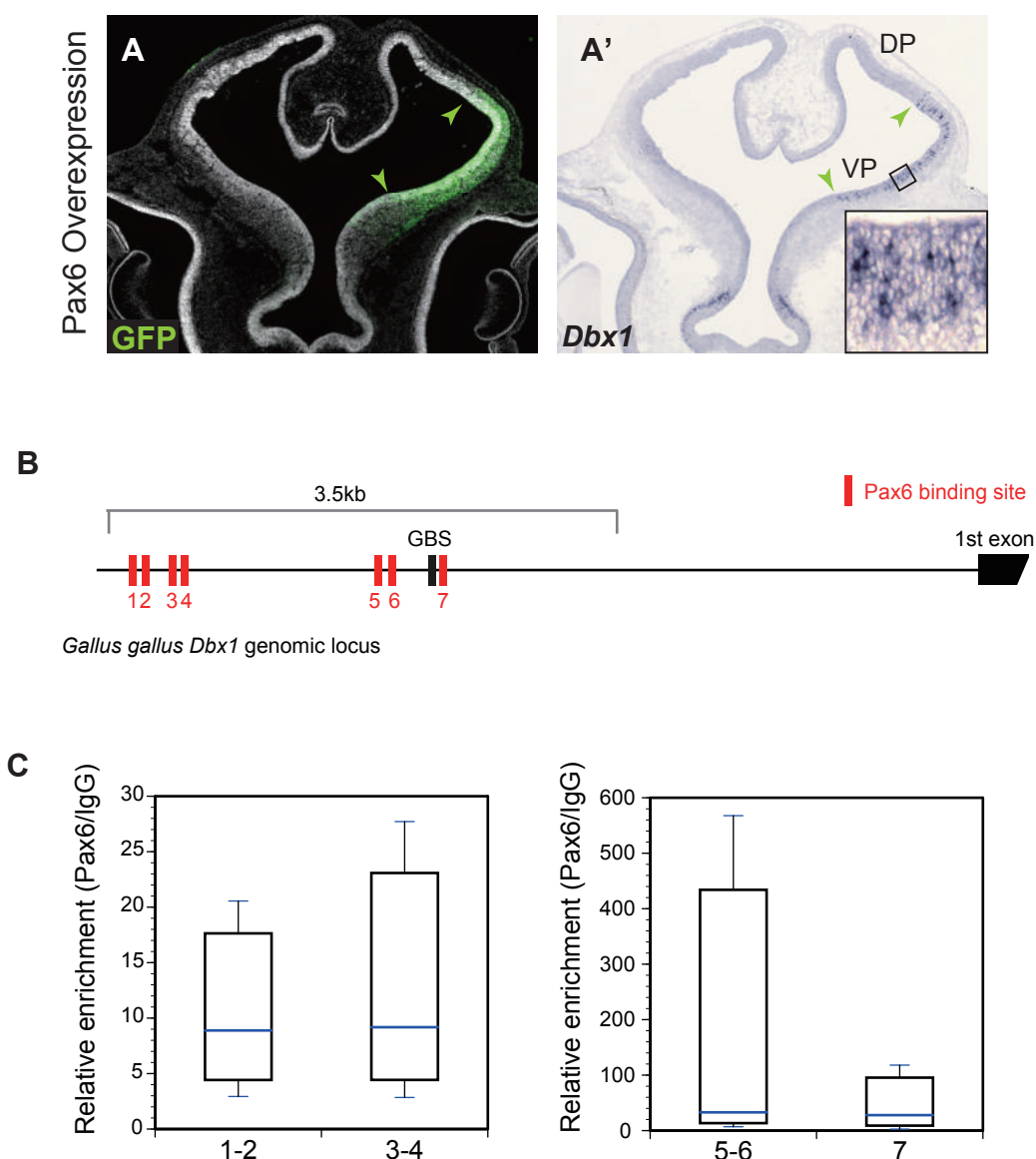
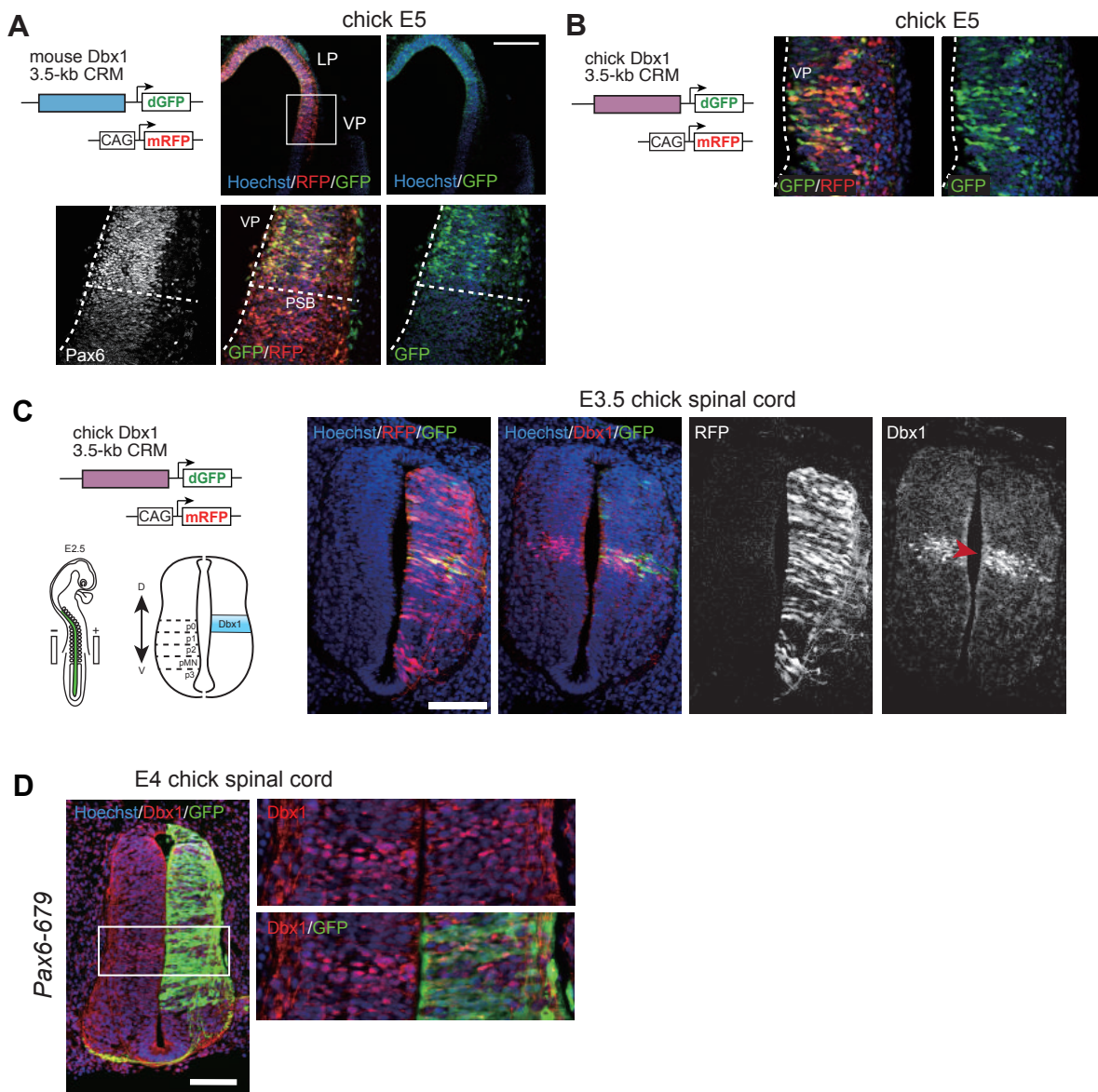


Fig. S6 (related to Fig. 4). Pax6-dependent activation of *Dbx1* and physical interaction of Pax6 on *Dbx1* 3.5-kb CRM

(A) Electroporation of Pax6 induces *Dbx1* expression in the developing chick ventral pallium (VP). (B) Distributions of putative Pax6 binding sites in chick *Dbx1* 3.5-kb CRM. GBS: Gli-binding site reported previously (Oosterveen et al., 2012). (C) ChIP-qPCR demonstrating relative enrichment of Pax6 binding sites (1-2, 3-4, 5-6 and 7) after immunoprecipitation with anti-Pax6 antibody.



test_id	gene_id	gene	locus	sample_1	sample_2	status	value_1	value_2	log2(fold_chang)	test_stat	p_value	q_value	significant
ENSGALG00000003965	ENSGALG00000003965	DBX1	5:2045882-2049582	control:lr2866_lr5275_lr5276	treatment:lr2867_lr5273_lr5274	OK	0.128984	16.3228	6.98355	6.42028	0.0002	0.0383213	yes
ENSGALG00000012941	ENSGALG00000012941	CDH12	2:73046217-7341333	control:lr2866_lr5275_lr5276	treatment:lr2867_lr5273_lr5274	OK	0.168492	3.4192	4.34291	4.43095	5.00E-05	0.0135907	yes
ENSGALG00000017485	ENSGALG00000017485	TLR1LA	4:69131052-69133509	control:lr2866_lr5275_lr5276	treatment:lr2867_lr5273_lr5274	OK	0.20848	3.80424	4.18963	3.79324	5.00E-05	0.0135907	yes
ENSGALG00000011115	ENSGALG00000011115	MME1	21:1387459-1411822	control:lr2866_lr5275_lr5276	treatment:lr2867_lr5273_lr5274	OK	0.216831	3.30088	3.92821	4.72478	5.00E-05	0.0135907	yes
ENSGALG00000005887	ENSGALG00000005887	PXDNL	20:9382941-9412831	control:lr2866_lr5275_lr5276	treatment:lr2867_lr5273_lr5274	OK	0.123655	1.74019	3.81485	3.94011	5.00E-05	0.0135907	yes
ENSGALG00000016138	ENSGALG00000016138	DSCAM	1:107601009-107978889	control:lr2866_lr5275_lr5276	treatment:lr2867_lr5273_lr5274	OK	0.133329	1.8734	3.81259	4.10264	5.00E-05	0.0135907	yes
ENSGALG00000017926	ENSGALG00000017926	7SK	3:87768166-87768495	control:lr2866_lr5275_lr5276	treatment:lr2867_lr5273_lr5274	OK	20.5253	248.4	3.59719	4.61408	5.00E-05	0.0135907	yes
ENSGALG00000003488	ENSGALG00000003488	PTPRT	20:3189961-3615919	control:lr2866_lr5275_lr5276	treatment:lr2867_lr5273_lr5274	OK	0.205108	2.11757	3.36795	3.56082	5.00E-05	0.0135907	yes
ENSGALG00000016448	ENSGALG00000016448	KCNF1	3:96578937-96581015	control:lr2866_lr5275_lr5276	treatment:lr2867_lr5273_lr5274	OK	0.226339	2.28174	3.33357	3.13143	0.0002	0.0383213	yes
ENSGALG00000009737	ENSGALG00000009737	taci	2:24773217-24779911	control:lr2866_lr5275_lr5276	treatment:lr2867_lr5273_lr5274	OK	1.20682	11.9954	3.31319	4.00289	5.00E-05	0.0135907	yes
ENSGALG0000003644	ENSGALG0000003644	-	10:3925575-3927300	control:lr2866_lr5275_lr5276	treatment:lr2867_lr5273_lr5274	OK	0.552565	4.57903	3.05083	3.24835	5.00E-05	0.0135907	yes
ENSGALG00000005246	ENSGALG00000005246	PAX3	9:7357517-7422566	control:lr2866_lr5275_lr5276	treatment:lr2867_lr5273_lr5274	OK	0.281772	2.32742	3.04613	3.08842	0.0002	0.0383213	yes
ENSGALG00000027381	ENSGALG00000027381	OLIG3	AADNO3015019.1:920-27	control:lr2866_lr5275_lr5276	treatment:lr2867_lr5273_lr5274	OK	1.36112	10.9275	3.00509	3.34019	5.00E-05	0.0135907	yes
ENSGALG00000012027	ENSGALG00000012027	SPON1	5:5838065-6002800	control:lr2866_lr5275_lr5276	treatment:lr2867_lr5273_lr5274	OK	2.33476	17.0096	2.865	5.03756	5.00E-05	0.0135907	yes
ENSGALG00000006003	ENSGALG00000006003	-	13:13158122-13161628	control:lr2866_lr5275_lr5276	treatment:lr2867_lr5273_lr5274	OK	0.336353	2.30225	2.77499	2.89816	0.00015	0.0337154	yes
ENSGALG0000002864	ENSGALG0000002864	LRRTM3	6:6129270-6562977	control:lr2866_lr5275_lr5276	treatment:lr2867_lr5273_lr5274	OK	0.484915	2.96387	2.61168	3.23203	5.00E-05	0.0135907	yes
ENSGALG00000027720	ENSGALG00000027720	OTX2	5:55680635-55688787	control:lr2866_lr5275_lr5276	treatment:lr2867_lr5273_lr5274	OK	1.08184	6.55973	2.60015	3.01196	5.00E-05	0.0135907	yes
ENSGALG00000005967	ENSGALG00000005967	-	5:9538612-9582720	control:lr2866_lr5275_lr5276	treatment:lr2867_lr5273_lr5274	OK	3.06274	17.8172	2.54038	3.51923	5.00E-05	0.0135907	yes
ENSGALG00000010133	ENSGALG00000010133	PTCH2	8:19696866-19712815	control:lr2866_lr5275_lr5276	treatment:lr2867_lr5273_lr5274	OK	1.10459	6.40092	2.53477	3.6027	5.00E-05	0.0135907	yes
ENSGALG00000013624	ENSGALG00000013624	FAM65B	2:9015385-90209672	control:lr2866_lr5275_lr5276	treatment:lr2867_lr5273_lr5274	OK	0.944413	5.28567	2.4846	3.31535	5.00E-05	0.0135907	yes
ENSGALG00000016035	ENSGALG00000016035	GFR4	4:88844983-88914622	control:lr2866_lr5275_lr5276	treatment:lr2867_lr5273_lr5274	OK	0.500423	2.77634	2.47196	2.86013	5.00E-05	0.0135907	yes
ENSGALG00000005519	ENSGALG00000005519	TLL2	6:16142743-16223667	control:lr2866_lr5275_lr5276	treatment:lr2867_lr5273_lr5274	OK	1.12504	5.26563	2.22663	3.06067	5.00E-05	0.0135907	yes
ENSGALG00000003541	ENSGALG00000003541	SLC32A1	20:4000629-4040091	control:lr2866_lr5275_lr5276	treatment:lr2867_lr5273_lr5274	OK	1.09842	4.83769	2.13889	2.56155	0.00015	0.0337154	yes
ENSGALG00000015419	ENSGALG00000015419	PENK	2:11076868-111081312	control:lr2866_lr5275_lr5276	treatment:lr2867_lr5273_lr5274	OK	3.87722	15.9351	2.03911	3.17814	5.00E-05	0.0135907	yes
ENSGALG00000010929	ENSGALG00000010929	SPARCL1	4:45106287-45113208	control:lr2866_lr5275_lr5276	treatment:lr2867_lr5273_lr5274	OK	2.86536	11.6232	2.02022	2.96313	5.00E-05	0.0135907	yes
ENSGALG00000003895	ENSGALG00000003895	PRDM12	17:5956540-5962675	control:lr2866_lr5275_lr5276	treatment:lr2867_lr5273_lr5274	OK	2.79254	11.284	2.01463	2.42497	0.00025	0.046381	yes
ENSGALG00000029020	ENSGALG00000029020	PPAPDC1A	6:30060585-30109050	control:lr2866_lr5275_lr5276	treatment:lr2867_lr5273_lr5274	OK	0.742306	2.9119	1.97188	2.59308	5.00E-05	0.0135907	yes
ENSGALG00000016749	ENSGALG00000016749	CNGA3	1:131289231-131309321	control:lr2866_lr5275_lr5276	treatment:lr2867_lr5273_lr5274	OK	2.52865	9.97982	1.95409	2.76615	5.00E-05	0.0135907	yes
ENSGALG00000020626	ENSGALG00000020626	PQLC2L	9:22146849-22157886	control:lr2866_lr5275_lr5276	treatment:lr2867_lr5273_lr5274	OK	4.99205	19.041	1.9314	3.1923	5.00E-05	0.0135907	yes
ENSGALG00000007588	ENSGALG00000007588	GAD2	2:16147742-16180423	control:lr2866_lr5275_lr5276	treatment:lr2867_lr5273_lr5274	OK	1.43714	5.09325	1.82539	2.60885	5.00E-05	0.0135907	yes
ENSGALG00000007361	ENSGALG00000007361	SS	9:14279798-14281333	control:lr2866_lr5275_lr5276	treatment:lr2867_lr5273_lr5274	OK	19.346	65.7312	1.76454	3.03532	5.00E-05	0.0135907	yes
ENSGALG00000012505	ENSGALG00000012505	LRFN5	5:59384567-59393956	control:lr2866_lr5275_lr5276	treatment:lr2867_lr5273_lr5274	OK	1.86441	6.29176	1.75474	2.32654	0.00015	0.0337154	yes
ENSGALG00000009415	ENSGALG00000009415	SMOC1	5:26991939-27112082	control:lr2866_lr5275_lr5276	treatment:lr2867_lr5273_lr5274	OK	1.74413	5.64102	1.69345	2.5928	0.0001	0.0254087	yes
ENSGALG00000023886	ENSGALG00000023886	ZNF804A	7:1771380-1902480	control:lr2866_lr5275_lr5276	treatment:lr2867_lr5273_lr5274	OK	3.91656	12.5334	1.67812	3.02459	5.00E-05	0.0135907	yes
ENSGALG00000006514	ENSGALG00000006514	FSTL4	13:15562923-15746366	control:lr2866_lr5275_lr5276	treatment:lr2867_lr5273_lr5274	OK	0.93563	6.09762	1.65544	2.28464	0.0002	0.0383213	yes
ENSGALG00000026592	ENSGALG00000026592	-	1:100373555-100373705	control:lr2866_lr5275_lr5276	treatment:lr2867_lr5273_lr5274	OK	3.255.21	10093.3	1.63257	3.02182	5.00E-05	0.0135907	yes
ENSGALG00000008263	ENSGALG00000008263	Far-1	12:17814859-1807537	control:lr2866_lr5275_lr5276	treatment:lr2867_lr5273_lr5274	OK	1.5951	4.92462	1.62637	2.7054	5.00E-05	0.0135907	yes
ENSGALG00000016709	ENSGALG00000016709	RCAN2	3:109338624-109369202	control:lr2866_lr5275_lr5276	treatment:lr2867_lr5273_lr5274	OK	7.4497	22.8787	1.61875	2.32006	0.0002	0.0383213	yes
ENSGALG00000016602	ENSGALG00000016602	ARHGAP6	1:123651001-123765375	control:lr2866_lr5275_lr5276	treatment:lr2867_lr5273_lr5274	OK	1.14284	3.47969	1.60633	2.32984	0.00015	0.0337154	yes
ENSGALG0000000750	ENSGALG0000000750	CAPN5	1:192455766-192506610	control:lr2866_lr5275_lr5276	treatment:lr2867_lr5273_lr5274	OK	1.34418	4.06355	1.59602	2.52612	5.00E-05	0.0135907	yes
ENSGALG00000011406	ENSGALG00000011406	NTN4	1:45466329-45505575	control:lr2866_lr5275_lr5276	treatment:lr2867_lr5273_lr5274	OK	1.42902	4.20594	1.5574	2.45542	0.0002	0.0383213	yes
ENSGALG0000001768	ENSGALG0000001768	TENM2	13:4187412-4738485	control:lr2866_lr5275_lr5276	treatment:lr2867_lr5273_lr5274	OK	4.3589	12.4201	1.51064	3.4309	5.00E-05	0.0135907	yes
ENSGALG0000002958	ENSGALG0000002958	DNER	9:9405231-9525036	control:lr2866_lr5275_lr5276	treatment:lr2867_lr5273_lr5274	OK	4.48093	12.5484	1.48563	2.50228	0.0001	0.0254087	yes
ENSGALG00000005176	ENSGALG00000005176	SCG2	9:7713654-7715544	control:lr2866_lr5275_lr5276	treatment:lr2867_lr5273_lr5274	OK	14.6951	35.348	1.26629	2.51991	5.00E-05	0.0135907	yes
ENSGALG0000000317	ENSGALG0000000317	NEFM	22:953201-957709	control:lr2866_lr5275_lr5276	treatment:lr2867_lr5273_lr5274	OK	8.04458	18.8846	1.23112	2.46643	5.00E-05	0.0135907	yes
ENSGALG00000012670	ENSGALG00000012670	NRSN1	2:58022131-58024847	control:lr2866_lr5275_lr5276	treatment:lr2867_lr5273_lr5274	OK	10.1155	23.4877	1.21534	2.27506	0.0002	0.0383213	yes
ENSGALG00000003193	ENSGALG00000003193	CRABP-I	10:3197349-3210246	control:lr2866_lr5275_lr5276	treatment:lr2867_lr5273_lr5274	OK	66.4452	150.042	1.17513	2.65086	5.00E-05	0.0135907	yes
ENSGALG00000009452	ENSGALG00000009452	GALNT16	5:27313855-2737424	control:lr2866_lr5275_lr5276	treatment:lr2867_lr5273_lr5274	OK	6.9461	15.3849	1.14724	2.5118	5.00E-05	0.0135907	yes
ENSGALG00000012620	ENSGALG00000012620	PTCH1	Z:41628097-41693685	control:lr2866_lr5275_lr5276	treatment:lr2867_lr5273_lr5274	OK	12.528048	11.3834	1.10819	2.35799	0.0001	0.0254087	yes
ENSGALG00000006258	ENSGALG00000006258	SPOCK1	13:13906201-14163956	control:lr2866_lr5275_lr5276	treatment:lr2867_lr5273_lr5274	OK	14.2906	30.6141	1.09914	2.50776	5.00E-05	0.0135907	yes
ENSGALG00000013357	ENSGALG00000013357	MTCL1	2:98628114-98720357	control:lr2866_lr5275_lr5276	treatment:lr2867_lr5273_lr5274	OK	6.57621	13.6063	1.04895	2.35061	5.00E-05	0.0135907	yes
ENSGALG00000006837	ENSGALG00000006837	TSPAN4	5:14631768-14696703	control:lr2866_lr5275_lr5276	treatment:lr2867_lr5273_lr5274	OK	20.0313	40.3151	1.00907	2.22582	0.0002	0.0383213	yes

mouse_Dbxi-3.5kb chick	CTTCCTGAAATACTTCTTCTGGCATTCA-TCTAGGCCAAAGGCTCAGCTATTGGGGC 881 CTCTTCTCAGTCAAAGCTCGGAAATCAAATATTGTATACTGCTTTCCAAAAGGC 1255 ** *
mouse_Dbxi-3.5kb chick	CC-CAGAGGCAGCTGTGGCACAGCAGGAGTGTTCCTCCATTCCAAGAAGCTCAA----- 934 CAGCACATGTAGTCTCCTCTGTGGATGCACTGCAGTTACAGAGACCTATGGATGA 1315 *
mouse_Dbxi-3.5kb chick	-----AGTGGAAAGTTTTTTTT-----TTTTTTTTTTTTTTAAGAGCTC- 979 GTACAGCAGTGGGTAGGGCTGTTCTGAAGAGATTACCACTGCCATTGGCAAACGATCA 1375 ***** *
mouse_Dbxi-3.5kb chick	-----TATGAAACAAACCTTTATCTCACCCATGGATCCACTGAGGCTGGGGGAAGAGG 1033 CCATTTGTGTTGCAGTCAGTAGGAGTAGTTGAAACCTGATTGGGGTGGGGG 1435 *
mouse_Dbxi-3.5kb chick	ACTTTCTTACAGAC-ACACCA--TAAGCGAACTCATGCAAACATGAGTTAAAGGCAA 1089 AATCCTTAATTCTCTGACCGACTTAGTGGAAACCAGAGAAGTACATGTTGGA-GAAAG 1494 *
mouse_Dbxi-3.5kb chick	GAACCTGGCTGGTAAGGCCTTGCCCCAACGCCAGATACCCGACTTCATTCTCAGGAC 1149 TAAGGAGGAAGGTA-TCACTTCCCTTGCTCTGAGGAAATTAGGCAAAGAATAAGT 1552 ** *
mouse_Dbxi-3.5kb chick	CCACCCATCTGGTAGGACAGAACCAAACCTCTGCCAGTTGCTCTGACTTACACACAC 1209 AC-TGTGTTGCACTCTGCAAACCCCAGCTCTCCAGTCACACACAACCCAGTCTGTGAAA 1611 *
mouse_Dbxi-3.5kb chick	ACACACACACAGAAAG 1269 GAAGCTGGCTTAGGGAGGTTCTGCATTTGATTGTTTATTAGCCAGATCAGTGGAG 1671 *
mouse_Dbxi-3.5kb chick	AGAGAGAGAGAGAGACTATTTAAATTCAAAGATTAGAATTAGGCAATCGAGGAAAAGA 1329 A-AGAAAGAAGGAGGATTGTTCAACCCCTGGAATATTACTATTTAAACAAAGAGTGGAGG 1730 *
mouse_Dbxi-3.5kb chick	GAAGGGAGTTATCTCAAGACTAAGAGTGTAACTTGAACCTAATTCTCAGATAAGG 1389 TTGGGAAACAGATAAA-AGGATGAGGTGGGAAAAATT--ATCATATCTGCAAGAAAGGG 1787 **** *
mouse_Dbxi-3.5kb chick	TGGTGGGGGATGGGGAGGTAGAGAAAG-CCACTGAAAGCCTCGCTCACCAA--CGTT 1446 TGCCAAGTAAACAGGGTAGGAAAGAGTTAGCAGGCTAACAGACAGGGACTAAAC 1847 ** *
mouse_Dbxi-3.5kb chick	TAATTTGATCATTCTCAGGGCTCTGATGTAUTGCCTAGCACTCTAGGGCTTGCATC 1506 TAAAGTAAATTACTCTGACAAGACGGGATCATCTGGTT-GCATTTAGGCCATGGCTC 1906 *** *
mouse_Dbxi-3.5kb chick	CCTGGGAAGGGGGGGCTCAGGGGACTACCAAGCCAGTACCACTGCACTGGCTGC 1566 TCTGGCTGGCCAGGATGAATGGTGAGGGAGAAGAAAGTAAC-TCTCCCCCTCAGGTCCC 1965 ***** *
mouse_Dbxi-3.5kb chick	CCTACAGAG---AGCCTTTCTTGAATTAAAAAAATTAAAAGAAAAAGAAAAAG 1622 TCTGCCAAGTCTGGGCCACGCTCTGCTCAAGATCCCTTTGCTCAGAGAGAGA 2025 *
mouse_Dbxi-3.5kb chick	AAAACACAAAAAAACACAACACAGTTAACCAACCTGTCAGGGCTGAGGATAACAATAAGG 1682 GAGGGGGAGAGGAGAGAGAACACAGTTAACCAACCTGTCAGGGCTGAGGACACAATAAGG 2085 *
mouse_Dbxi-3.5kb chick	GCCTTGAAAAAGAGCTTTCATGCATGCCTAATATATTGTTAGCTATTCACTTAATG 1742 CAGCCCCAAAAGAGCTTTTCATGCATGCCTAATATATTGTTAGCTATTCACTTAATG 2145 ***** *
mouse_Dbxi-3.5kb chick	AAGCTGATCAATGTGATGGGAGACAATGGTCAAGTTAATCTATTAGTAAATGTTG 1802 AAGCTGATAATGTGATGGCAGAACATAGTCAGTTAATCTATTAGTAAATGTTG 2205 ***** *
mouse_Dbxi-3.5kb chick	GACTTTCAGGCTATGAGAAGGAGGGAGCCT--TTGGCGACATTTCATTAAATAAC 1860 GACTCTCAGGCGATGTTAAGGAGGGTAGTGTGTTAGGGACATTTCATTCAATA-CTC 2264 ***** *
mouse_Dbxi-3.5kb chick	TCCTCTCTTCTAGGCTGCACAAGGGGGTTCAGGCAATCTATGTAATATAATTCTTATA 1920 TCATCTCTCCC--CTCTTAGGGGGTTCAGGCAACCTATGTAATATAATTCTTATA 2321 ** *
mouse_Dbxi-3.5kb chick	AACGTGTCTTAATGGGTTAATTCCACCTTGCAGCTGTTGGGAGCTATTGTAAG 1980 AATGTGTCTTAATGGGTTAATTCCACCTTGCAGCTGTTTTAGCTATTGTAAG 2381 ***** *

mouse_Dbxi-3.5kb chick	AAGGGTCTATGTGGATCATGAACGGGTAGACCTACCTTATACTGAGTCAGGTGGCCTCG	3293
mouse_Dbxi-3.5kb chick	TAAAAAACAGAGCTTAGATACGTTGGATTGTGGAGAGCAAAACTGCCGGAGGATGAGGA	3353
mouse_Dbxi-3.5kb chick	GGGTAGCTAGCCTTCCAGGGCTGCAGAAACCACACCTCCACGGAAAGTAACCTCGGGAGGC	3413
mouse_Dbxi-3.5kb chick	GGGACCTGGGAAGACCCACTGTGCTGTCTAATCTTTCTTGGCAGAAACCTAGCG	3472

Table S2. Sequence comparison of mouse and chick Dbx1-3.5kb CRMs.

Pair-wise sequence alignment was performed by CLUSTALW. Asterisks represent conserved sequences. Putative Pax6-binding sites are represented in red (see also Figure S6B). A Gli-binding site (Oosterveen et al., 2012) is shown in green.

List of primers used for qPCR

Target	Forward primers	Reverse primers
beta-actin	CAGACATCAGGGTGTGATGGT	TCCTCAGGGCTACTCTCAG
Ccnd1	CTTGGATGCTGGAGGTCTGC	CTGCGGTAGAGGAATCGTT
Cdk6	GGCCTAATGATGTGCCCTT	TCTTGGCTGGATTGAACGCT
p27 ^{Kip1}	GCCGACGATTCTCTCCTCAAAA	ATCTTCCTGGCTTCACCGCC
Notch1	GAGCAGAGAGGGATGAAGCG	CACTGCTGCACTGGCACA
Dll1	TTCGGTCACTTCACCTGTGG	ACCCACTCTGCACTTGCATT
Dbx1	CAACCGAATTCCCAGCTATT	GGACAGTGGTTGTCTGCAC

List of primers used for pX330 plasmid construction

	Forward primers	Reverse primers
pX330-Pax6-347	CACCGCGCGGTGAACCAGCTCGGCG	AAACCGCCGAGCTGGTTCACGCCGC
pX330-Pax6-679	CACCGAGACAGATTACTCTCGGAG	AAACCTCCGAGAGTAATCTGTCTC
pX330-Pax6-811	CACCGGATGCTGAACGGGCAGACG	AAACCGTCTGCCGTTCACGCATCC

List of primers used for isolation of Dbx1-CRM

Target	Forward primers	Reverse primers
Mouse 3.5 kb-CRM	CTGAGAAGGCTGGAAGAG	CGCTAGGTTCTGCCAAG
Chick 3.5 kb-CRM	CCTGTCTCCCTAAAGAGTTATACC	CGATGCGTCTGAGCACACTCGT

List of primers used for ChIP-qPCR

Target	Forward primers	Reverse primers
BS1-2	ATGCCAATTGCATCATAGCC	TCCTGGAATAGGACCAACAGG
BS3-4	AGGCTAAAGCTACGGGAAA	TGACAAGCAGGAAGAAATGC
BS5-6	GAGGATTGTTCAACCCTGGA	GATGATCCGTCTTGTCAAGAA
BS7	GAGGGGGAGAGGGAGAGAA	TTTCGCATCACATTATCAGC

Table S3. Primers used for qPCR, pX330 plasmid construction and ChIP-qPCR

Supplementary references

Oosterveen, T., Kurdija, S., Alekseenko, Z., Uhde, C. W., Bergsland, M., Sandberg, M., Andersson, E., Dias, J. M., Muhr, J. and Ericson, J. (2012). Mechanistic differences in the transcriptional interpretation of local and long-range Shh morphogen signaling. *Dev Cell* **23**. 1006-1019.